

## Article

# Damage Assessment of Road Bridges Caused by Extreme Streamflow in Montenegro: Reconstruction and Structural Upgrading

Jelena Pejović \*, Nina Serdar  and Radenko Pejović

Faculty of Civil Engineering, University of Montenegro, 81000 Podgorica, Montenegro; ninas@ucg.ac.me (N.S.); radenko@ucg.ac.me (R.P.)

\* Correspondence: jelenapej@ucg.ac.me

**Abstract:** The extreme river streamflow that occurred during floods in 2010 in Montenegro caused significant damage to infrastructure and road facilities. The most severe damages were located on bridges crossing the river Lim, where a rapid water level increase in several municipalities led to failure or damage of almost 20 bridges. In this paper, a damage assessment of four significantly damaged reinforced concrete (RC) bridges, located in the affected zone of 40 km, is conducted. One bridge in Berane (bridge 1) and three bridges located on roads upstream from Berane (bridges 2, 3, and 4) were analyzed. Extreme water levels and inadequate flow profiles caused great damage to the bridges of which the piers were not adequately founded. A scouring process under the foundation of piers and abutments located in the riverbed occurred due to surface erosion and degradation of alluvial sediments. Applied methods and techniques for reconstruction and structural strengthening of bridges are presented in detail as well as results of conducted analyses of the design reconstruction process. In order to design appropriate structural strengthening, nonlinear analyses of bridges due to the settlement of the piers were performed. The research findings can be used in the vulnerability assessment and reconstruction planning phases for other bridges in the considered zone.

**Keywords:** RC bridges; damage state; floods; extreme streamflow; reconstruction; structural upgrading; nonlinear analysis; plastic hinge



**Citation:** Pejović, J.; Serdar, N.; Pejović, R. Damage Assessment of Road Bridges Caused by Extreme Streamflow in Montenegro: Reconstruction and Structural Upgrading. *Buildings* **2022**, *12*, 810. <https://doi.org/10.3390/buildings12060810>

Academic Editor: Beatrice Belletti

Received: 21 April 2022

Accepted: 8 June 2022

Published: 12 June 2022

**Publisher's Note:** MDPI stays neutral with regard to jurisdictional claims in published maps and institutional affiliations.



**Copyright:** © 2022 by the authors. Licensee MDPI, Basel, Switzerland. This article is an open access article distributed under the terms and conditions of the Creative Commons Attribution (CC BY) license (<https://creativecommons.org/licenses/by/4.0/>).

## 1. Introduction

Bridges are the most vulnerable structures of transport infrastructure, exposed to multiple natural hazards, with flooding being the leading cause of bridge failures in the world [1]. Their performance is constantly influenced by different combined effects such as impacts of natural hazards (floods, earthquakes), aging, increasing traffic loads, and aggressive environmental conditions. The most severe recorded damages to bridges are hydraulically induced and particularly caused by scouring that is activated by floods [2]. Additionally, bridges located in earthquake-prone and flood-prone regions, such as Montenegro, can be exposed to flood-induced scouring in combination with seismic events, resulting in a potential increase in the structure's vulnerability [3–11].

One of the most common causes of bridge pier stability loss is local erosion (local scour) in the foundation pier zones [12]. Local erosion involves the removal of material around bridge piers. It is caused by the local acceleration of water when it encounters a kind of obstacle that leads to turbulence and vortex. This matter is especially pronounced in torrential water flows, given the high speeds of water flow and the significant amount of sediment they carry with them. Large amounts of sediments carried by torrential water flows (together with branches and trees) during a flood wave can deposit and block the bridge's free flow profile, reducing its capacity, thus creating hydraulic conditions conducive to increased erosion at the site of the pier foundation. Some studies pointed to the fact that the formation of sediment deposits is one of the main causes of bridge stability

loss, where in one-third of the total number of analyzed bridge collapse cases across the UK, Ireland, and the USA, this effect was of the greatest importance [13]. In the USA, hydraulic actions such as scour process have been recognized as the most disastrous causes of bridge failures, representing more than 50% of the cases [14,15]. Based on a record of scour-induced failures in the UK over a period of 173 years, it is estimated that the annual probability of bridge failure is 27%, i.e., one out of three river bridges might be damaged due to flood [1]. During the 2014 floods in Serbia, 307 bridges were damaged, and the total losses for transport infrastructure were estimated to be €166.5 m, with a reconstruction cost of €128 m [1,16]. In literature, extensive research is done related to scour actions to the bridges including numerical studies [17–20] and monitoring studies [21–23].

Previously conducted studies on damage assessment analysis of the existing RC bridges in Montenegro [24–29] have shown that the most common causes of bridge damages are due to design or construction errors, especially pronounced in the conditions of exposure to natural hazards, inadequate bridge maintenance, and unfavorable exploitation conditions. These studies are focused on bridges in Montenegro that have been designed more than 40 years ago, when the design provisions related to structural durability were significantly less rigorous than required [30,31]. The bridges from that period were designed to be rational from the aspect of material usage leading to the adoption of minimal concrete covers [24,25,30], lower concrete strength classes, or inadequate reinforcement arrangements compared to present provisions. The conducted analysis on damaged bridges showed that RC slabs are designed with a thickness in the range of 0.15 to 0.18 m in the middle of the spans. Under severe exploitation conditions these RC slab thicknesses were insufficient and over time, severe damages occurred, or in some cases, even their complete structural failure [24]. Damage to RC slabs was initially reflected in the appearance of concrete cracks and/or spalling and reinforcement corrosion, then the process has intensively continued and resulted in complete failure of the slab (formation of holes in the slab) [24]. The relatively thin concrete covers, that additionally were not specifically controlled in the construction stages, leading to their poor quality caused the rapid corrosion of reinforcement and spalling of larger concrete cover areas, after which the process continuously progressed [25]. A lot of existing studies have been conducted in the area of corrosion's influence on the reduction of the bearing capacity of the structural elements [32–39]. It is worth mentioning that the older bridges were designed according to the former/existing regulations for the design of bridges [31,40], while the Eurocodes provisions in bridge design are relatively recent [41–43]. Bridges that are calculated according to the old regulations generally cannot meet the conditions prescribed by the new regulations, which is why their structural strengthening is needed [26,27]. An example of such a case is the road bridge in the center of Podgorica across the river Moraca [26], whose reconstruction required structural upgrading in order to increase its structural bearing capacity for the higher traffic load values. A new layer of concrete with an average thickness of 13 cm over the existing slab was needed as well as additional reinforcement and carbon strips in RC girders and slab to meet the required capacity conditions. Further, from past studies, the significant damages in the bridge's support zones and hinged connection zones were noticed due to the small bearing lengths provided. Moveable supports of older bridges are usually concrete bearing quads that are highly damaged, and they must often be replaced with modern bearing systems [25]. The use of hinged connections in bridge structures has proven to be their weak point, where serious damage occurs [28]. In addition, the most common construction errors were related to the quality and concrete installation. Preliminary sampling and testing of concrete have not been mandatory, which aim to ensure the durability and appropriate concrete workability by technological criteria, but standard concrete mixtures are used, characterized only by the concrete class [30]. The problem for small dimension RC sections with closely spaced reinforcement was providing the compactness of the placed concrete, which is why segregation often occurred [28,29].

Furthermore, frequent damage to bridges in Montenegro occurred due to the scour that is caused by extreme river streamflow. In the scour process, the settlement of the

bridge foundation occurred most often since bridges were inadequately founded, i.e., they were not founded on solid rock (if it was at an acceptable depth) or on piles, but shallow foundations were placed in the riverbed on the gravel material. The mountain torrential water flows with high water level oscillations present a particular danger for bridges in Montenegro. These torrential water flows can carry branches and trees that make a floodgate with great destructive action of water in the bridge zone [29,44,45].

At the end of 2010, in November and December in Montenegro, in the territory of the Lim River valley, extensive rainfall occurred that caused severe flooding: the entire regions were flooded, especially those along rivers and lakes. In the first wave, as a result of four rainy days, the floods began on November 9 and lasted for 5 days. After a short-term stabilization of weather conditions, new rainfall from 17 November to 5 December followed, which caused a new wave of floods. The floods and extreme river streamflow caused great damage to infrastructure facilities, road facilities, embankments, etc. Traffic on some roads was interrupted due to floods. The greatest damages were caused by the river Lim with a sudden rise in water levels (water level maximums were recorded) at the municipalities of Plav, Andrijevica, and Berane. The Lim River, with its tributaries and an extremely large catchment area, has extreme fluctuations in water levels. Thus, the Lim River in Plav has a minimum flow  $Q_{\min} = 1.5 \text{ m}^3/\text{s}$ , and a maximum flow  $Q_{\max} = 324 \text{ m}^3/\text{s}$ , where the ratio is 216, and in Berane  $Q_{\min} = 4.2 \text{ m}^3/\text{s}$ , and  $Q_{\max} = 655 \text{ m}^3/\text{s}$ , where the ratio is 156. Such variations in the flow given by the ratio between the minimum and maximum flow, classify the Lim River as a torrential water flow that can have a significant negative impact on the environment. The consequences of such a devastating effect of the Lim River, among others, are that in the area between Berane and Plav, about 20 bridges were destroyed and/or damaged, with estimated damage in the amount of several million euros [46].

Since no comprehensive study on the vulnerability of existing deteriorated bridges to the extreme river stream conditions was conducted in Montenegro, although almost 60 bridges have been built in the Lim River basin area [46], the study presented in this paper partially fills this gap. The objective of this research is to detect the most important design and construction flaws related to the period of intensive construction of bridges in Montenegro. The aim is to determine bridge vulnerable components and possible failure modes for the extreme river stream conditions as well as to present possible retrofitting solutions based on the selected representative bridges. The study tries to facilitate retrofitting design of damaged bridges by justifying the selection of a new structural system with hinges inserted in zones where significant damage was observed. The selected representative bridges are prototypes, adequately representing the bridges in the considered zone.

Four significantly damaged bridges are analyzed, all located in the affected zone of 40 km (Figure 1). The damaged city bridge Niko Strugar in Berane (bridge 1), as well as three bridges on local roads upstream from Berane, were analyzed: Marsenic bridge at the Marsenic River site in the municipality of Andrijevica (bridge 2), the Seoca bridge also in the municipality of Andrijevica (bridge 3) and the Novsici bridge in the municipality of Plav (bridge 4). Figure 2 shows the flow of Lim in the area of the Marsenic bridge. The total damage to those three bridges is estimated at around €1.2 m. In this paper, a detailed description of damages and designed reconstruction measures for four damaged bridges (bridges 1–4) are presented. The bridge damage assessment is also checked by conducting a nonlinear analysis, the results of which are presented here, as well as the description of applied methods and techniques for reconstruction and structural upgrading.

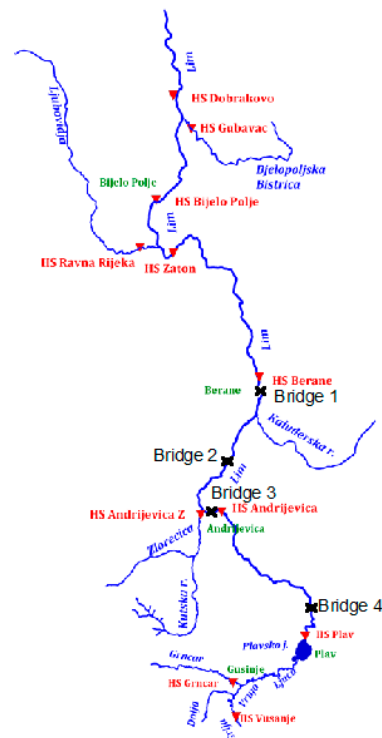


Figure 1. Lim River with positions of damaged bridges.



Figure 2. Lim River water level in the area of the Marsenic bridge.

## 2. Materials and Methods

Due to missing or incomplete design documentation for the considered bridges, it was necessary to conduct additional on-site tests to determine the characteristics of the material. Where relevant (bridge 1 and bridge 2), the compressive strength of concrete in the RC deck was determined by extracting and testing four cylindrical concrete specimens from the bridge deck with a diameter and height of 0.10 m. For bridge 1, all specimens showed the high quality of the existing concrete, i.e., compressive strength exceeding 50 MPa or an average of 55.51 MPa. For bridge 2, the compressive strength is 25 MPa, although the designed compressive strength was 30 MPa. Further, it was determined that the smooth reinforcement has been used with a characteristic tensile strength of 360 MPa and a yield strength of 240 MPa. Concrete and steel mechanical properties were in line with national

provisions valid at the time of bridge construction [30]. The smooth reinforcement is not acceptable according to present standards [41], as are deck concrete strengths lower than 45 MPa. The quantity and arrangement of reinforcement bars were determined by the on-site reinforcement detection method.

To confirm the real damage state of the bridges, inspect failure modes, and justify the use of a new structural system in structural strengthening design, a nonlinear analysis of bridges 1 and 2 was conducted. Bridges are modeled as spin line models, using single line beam elements to represent bridge deck (only bridge deck is modeled), in the software package Seismostruct [47]. Nonlinear behavior is expected to occur in the deck section, so inelastic frame displacement-based elements (infrmDB), which follow a standard FE approach from [48,49], are used to model the deck. These 3D elements are used to model space frames with geometric and material nonlinearity. Cross-sections are divided into 400 individual fibers where each fiber has a defined corresponding uniaxial material response. Stress-strain state is obtained by integration of material responses of those fibers accounting for inelasticity across member length and section depth. The material of unconfined concrete and the material of confined concrete are defined for the section concrete cover and core, respectively. Mander model [50] is used to model confined concrete. Reinforcement steel and cyclic behavior are modeled using [51]. Eight elements are used to model the first and last spans, and nine elements are used per inner two spans in the case of bridge 1. Ten elements are used to model the first and last spans, and sixteen elements are used for the inner span in the case of bridge 2. For bridge 2, prestressing is modeled as equivalent load acting as permanent load. Inelastic elements are placed at the cross-section centroids. At the location of abutments, as well as piers, elastic rigid elements are used to model the connection of the deck centroid and pier top. The stiffness of the rigid elements is assumed to be 100 times the stiffness of the adjacent elements. At the end of these elements, zero-length link elements are employed to model soil flexibility in global Z-direction and restraint conditions, with adopted values for partial fixity in link elements. Foundation settlement is employed as an incremental load that represents a pseudo-static load in terms of displacements. The magnitude of displacement is changed in every step of the analysis by multiplying the nominal value of 0.01 m and load factor (in this case equal to step number). A total of 70 loading steps are conducted. In each step of the analysis defined performance criteria are checked: the reinforcement yield and the chord rotation capacity.

### 3. Damage Assessment of Niko Strugar Bridge (Bridge 1)

#### 3.1. Description of Bridge Structure

The Niko Strugar bridge is located in the city of Berane. It was built in 1965. The bridge is an RC bridge with a continuous deck system with four spans: 24.60 m, 27.60 m, 27.60 m, and 24.60 m. The total length of the bridge is 104.40 m. The width of the bridge is 10.46 m with two traffic lanes 3.57 m wide and two footpaths 1.66 m wide. The longitudinal bridge section in the axis of the bridge and deck cross-section in the middle of the spans are shown in Figures 3 and 4. The bridge deck consists of two pairs of adjacent girders 0.36 m wide, placed at a distance of 1.14 m. The girders are variable in height: 1.60 m in the middle of the span, and 2.20 m at the supports, including the RC slab thickness. A girder's height is changed linearly from the supports at the inner bridge piers over the length of 5.90 m on both sides, while at the rest of the span, the length height is constant. At the length of the variable girder height, the pairs of adjacent girders are connected by a flange 0.15 m thick at the bottom edge. The bridge has transverse girders at the supports and in the spans. Over the abutments, the cross-section dimensions of transverse girders are  $0.50 \times 1.60$  m, over the inner supports  $0.25 \times 2.20$  m, and in the spans  $0.25 \times 1.05$  m. The transverse girder's distance is 4.60 m along the spans, except for the first ones, which are placed at a distance of 6.20 m from the abutments. The RC slab is 0.20 m thick with a linear increase in thickness to 0.40 m at connections to the longitudinal and transverse girders along the length of 0.20 m. Footpaths are carried by cantilevers 1.50 m long. The thickness of the cantilever is 0.40 m at the fixed end, and 0.20 m at the free end. There is a

0.06 m thick layer of asphalt over the RC slab. The river piers are massive concrete elements with a depth of 1.20 m, 9.45 m width, and 5.95 m height, semi circularly rounded in the direction of the river flow. The foundations of river piers are shallow foundations with dimensions of  $2.16 \times 10.44$  m in-plane, while the height of the foundation could not be determined on-site since the original project documentation was missing. The abutments are also massive concrete elements with dimensions that could not be determined on-site except for the width. The wing walls of the bridge are parallel. Over the left abutment is a fixed bearing, while over the other supports moveable bearings of the concrete pendulum system were designed.

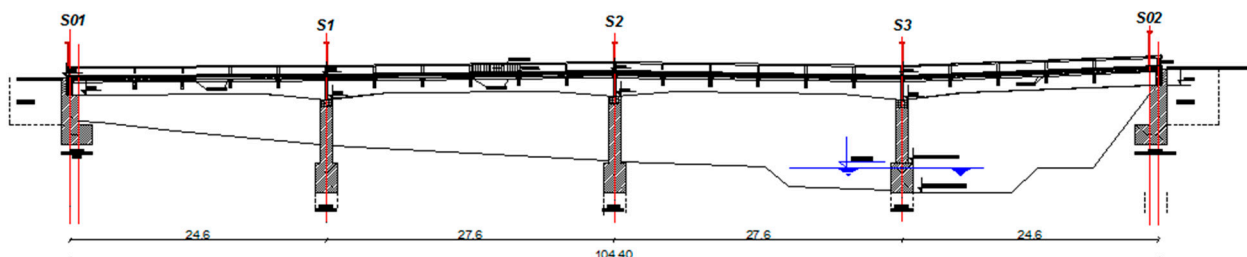


Figure 3. Longitudinal section of the bridge.

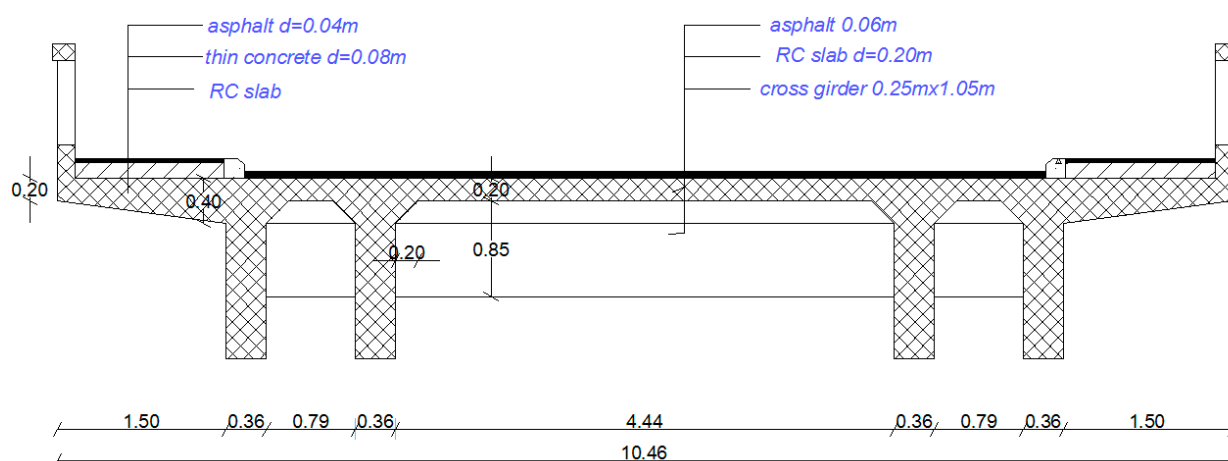


Figure 4. Bridge deck cross-section in the middle of the spans.

The longitudinal girders have bottom reinforcement of  $14\phi 36$  in the middle of the spans (placed in three layers). The concrete cover to the reinforcement is 0.03 m, and the clear spacing of the bar layers is 0.036 m. Transverse reinforcement (stirrups) are  $\phi 12/0.20$  m. At the supports in the upper zone of the sections, the longitudinal girders are reinforced with  $17\phi 36$ . In the middle slab spans, the reinforcement is  $\phi 12/0.10$  m in both directions, while in the end slab its span is  $\phi 14/0.10$  m. In both directions at the middle supports, the reinforcement is  $\phi 12/0.05$  m. The concrete cover to the reinforcement in the slab is 0.02 m. All concrete covers were in line with national provisions valid at the time of bridge construction [30], which is up to 0.025 m lower concrete cover thickness according to present provisions [41].

### 3.2. Description of Bridge Damage

Due to extreme river streamflow, the settlement of the river pier S3 of 0.64 m occurred (based on the geodetic measurement of the deformed bridge), which caused serious damage to the bridge structure (Figure 5). In the span between piers S3 and S02 next to the S3 river pier, at a distance of 3.3 m (zone 1), the deck collapsed. In the longitudinal girders, the cracks about 15–20 mm opened in the bottom zone, while the concrete in the upper zone on the part of footpaths was crushed. At these sections, the concrete of the RC slab was

also crushed. With this level of displacements, it is reasonable to assume that the yield of reinforcement and the plastic hinge formation occurred. In the span between S2 and S3 next to the pier S2, at the distance of 2.35 m (zone 2), damage was also observed. At this section, cracks appeared in the upper zone, while no crushing of concrete was observed in the bottom zone of the longitudinal girders.



**Figure 5.** (a) The bridge after the settlement of the river pier and (b) cracks in zone 1.

Based on the visual inspection and geodetic survey, it was also observed that the pier S3 uniformly settled in both, the longitudinal and transverse directions. The pier S3 settled due to erosion and degradation of alluvial sediments under the water flow. During the field investigation conducted by diving, it is concluded that scouring occurred at the peripheral parts of the bridge pier foundation and that the pier was supported only by the central part of the foundation.

### 3.3. Nonlinear Analysis of the Bridge 1 Due to the Settlement of the River Pier S3

In order to design the appropriate structural strengthening of the damaged bridge 1 as well as to obtain a real distribution of action effects in the bridge 1 for the new damage state, a nonlinear analysis of the bridge 1 due to the settlement of the river pier was performed. A schematic representation of the model is shown in Figure 6.



**Figure 6.** Schematic representation of bridge 1 nonlinear model (\*, \*\* nodes at the bents).

#### 3.3.1. Element Forces during the Analysis

Bridge bending moment diagrams in the downstream girder for several settlement values under the pier S3, including permanent gravity loads, are presented in Figure 7b,c. The initial state shown in Figure 7a refers to permanent gravity loads acting on the deck structure.

As expected, the increase in negative bending moments at the cross-section above pier S2 up to 3 times, as well as a decrease in the negative bending moments at the sections near pier S3 and even their transformation to the positive moments for the significant values of settlement is noticed. The bending moment at the bottom edge in the last span (S3-S02) also increased up to 2.4 times.

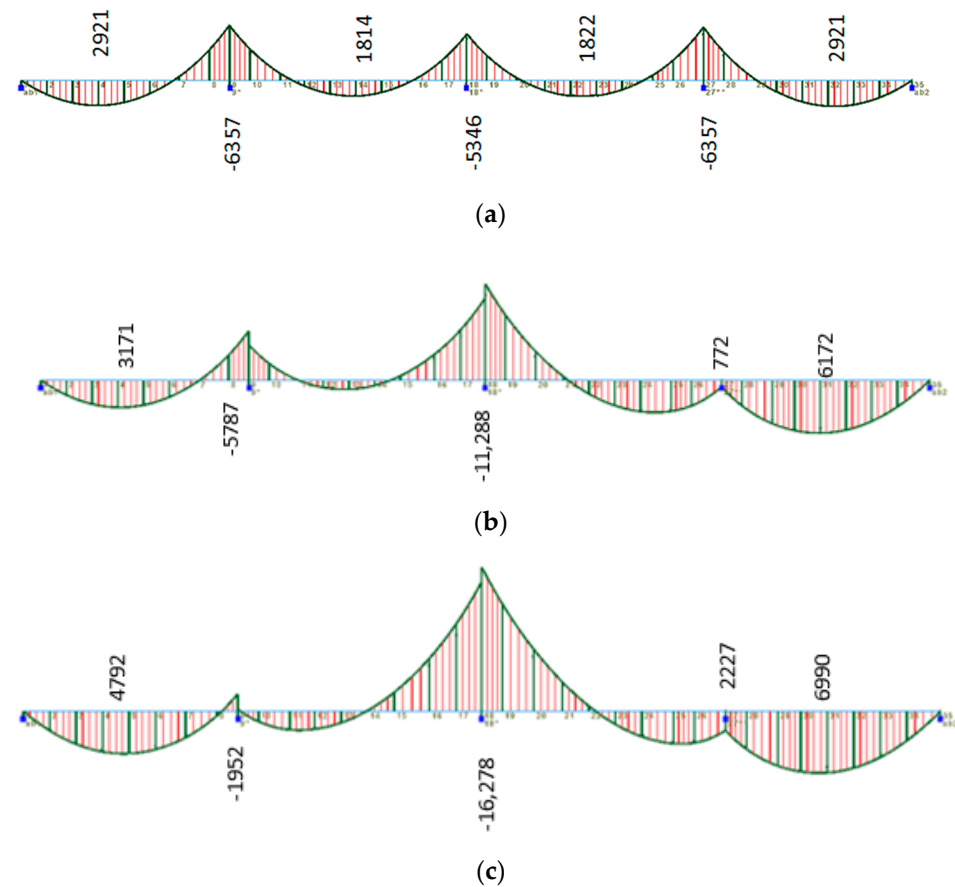


**Figure 7.** (a) Bending moment diagram—initial state (units in  $\text{kN}\cdot\text{m}$ ). (b) Bending moment diagram—settlement of 0.14 m under S3 (units in  $\text{kN}\cdot\text{m}$ ). (c) Bending moment diagram—settlement of 0.71 m under S3 (units in  $\text{kN}\cdot\text{m}$ ). (\*, \*\* nodes at the bents).

### 3.3.2. Element Deformation and Performance Check

During the loading phases, two performance criteria are defined: the reinforcement yield and the chord rotation capacity. The reinforcement yield is considered to be reached when reinforcement strain exceeds the value of 0.0012. The chord rotation capacity is calculated based on EN 1998-3:2005 Annex A [52]. The load is applied as displacement below the pier S3 that simulated the foundation settlement in steps of 0.01 m. The results show that reinforcement yield occurred in the next order: (1) at node 28 located 2.35 m from pier S3, at the settlement of S3 pier of 0.14 m; (2) at node 20 located 5.9 m from pier S2, at the settlement of S3 pier of 0.48 m, and (3) at node 18 located above S2, at the settlement of S3 pier of 0.65 m. Chord rotation capacity was reached at node 28 for settlement of S3 pier equal to 0.71 m. Figure 8a–d shows a schematic bridge deformed shape at the analysis step when checked performance criteria are reached.

Figure 9 shows the bending moment-rotation diagrams for nodes 28, 20, and 18. The points of reaching performance criteria are marked on the charts.

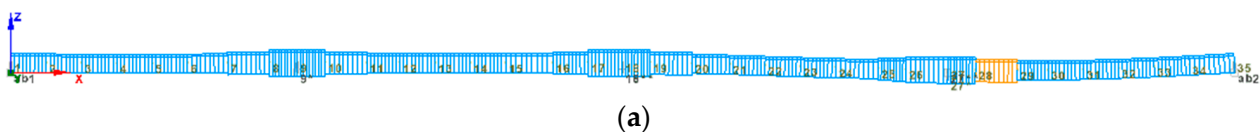


**Figure 8.** Cont.

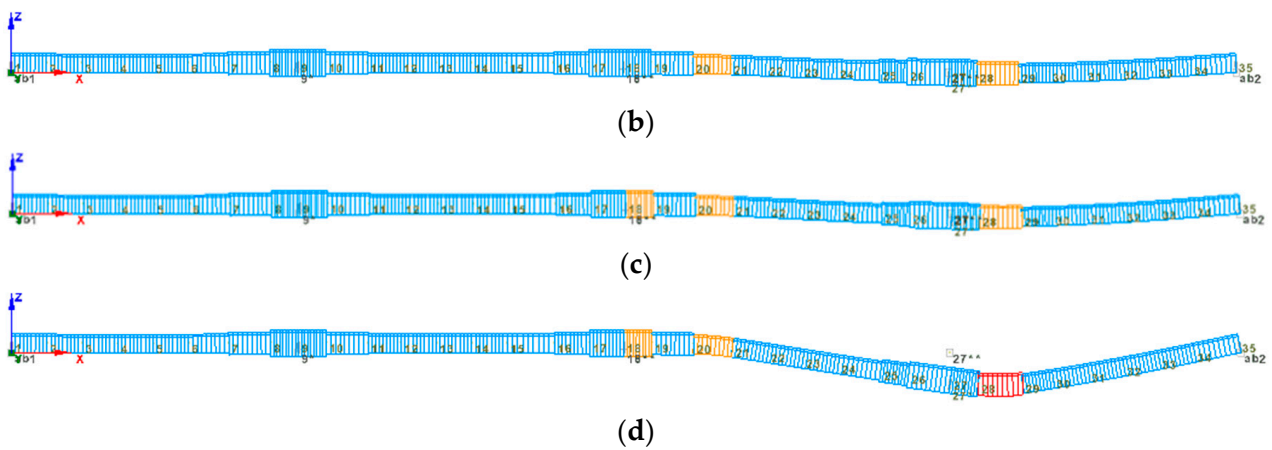
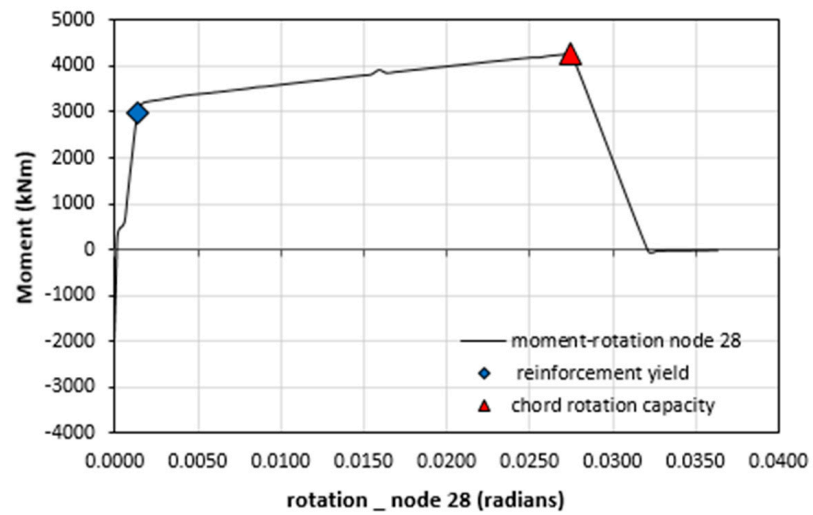
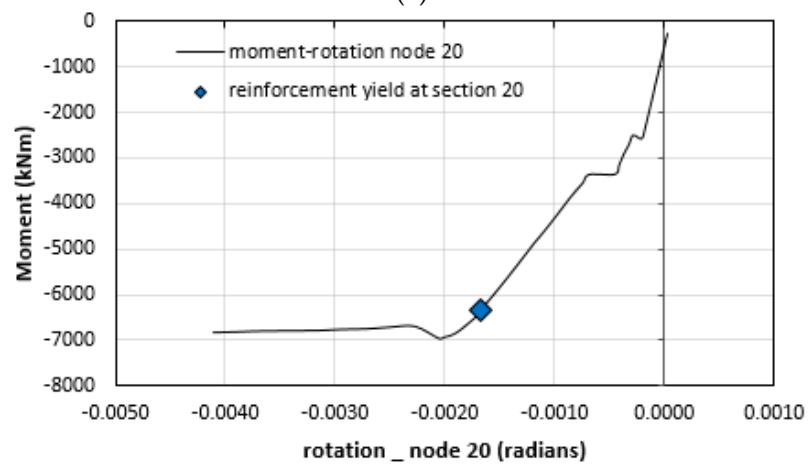


**Figure 8.** (a) Step 15: the reinforcement yield at 2.35 m from S3 pier for 0.14 m settlement of S3 pier. (b) Step 49: the reinforcement yield at 5.9 m from S2 pier for 0.48 m settlement of S3 pier. (c) Step 66: the reinforcement yield above S2 pier for 0.65 m settlement of S3 pier. (d) Step 72: the chord rotation capacity reached 2.35 m from S3 pier for 0.71 m settlement of S3 pier. (\*, \*\* nodes at the bents).

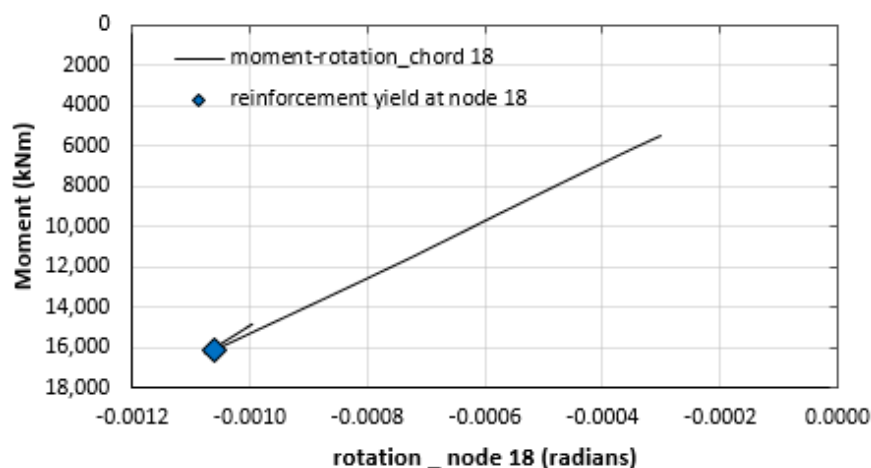


(a)



(b)

**Figure 9.** Cont.



(c)

**Figure 9.** Moment rotation curve for nodes (a) 28, (b) 20 and (c) 18.

From the shown results, it can be noticed that after the first yield, the bridge section located at 2.35 m from S3 (corresponding to model node 28) exhibited significant nonlinear behavior. Yielding of longitudinal reinforcement occurred at a section located 5.9 m from S2 (corresponding to model node 20). As the settlement increases, the bridge deck section above pier S2, corresponding to node 18, mostly shows elastic behavior. Additionally, after the point of reaching the first yield in this section until the settlement S3 pier of 0.71 m, a small increase in moments is noticeable.

At the analysis step that corresponds to the settlement of S3 pier of 0.71 m, chord rotation capacity (value of 0.02750126 rad) was reached at the section located 2.35 m from S3 pier. At this step, rotation of node 20 of 0.00226645 rad is reached which is 1.36 times more than rotation at first yield.

It can be concluded that sections in which significant reinforcement yielding occurred in a nonlinear model (zones of nodes 28, 18, and 20) correspond to the cross-sections in which the damage occurred in the bridge (zone 1 and zone 2). In the zone of node 28 corresponding to zone 1 of bridge damage, the rotation capacity was reached, which clearly indicates the complete plastification of the plastic hinge. This was obvious from in situ bridge damage in zone 1 where the cracks about 15–20 mm wide opened in the bottom zone, while the concrete in the upper zone was crushed. In zone 2, where less damage was occurred compared to zone 1 (in the form of cracks in the upper zone, while in the bottom zone no crushing of concrete was observed in the main girders), the plastic hinge formation occurred but rotation capacity was not reached (10% of the rotation capacity was reached). This state of damage also corresponds to in situ bridge damage. Since the rotation capacities were exceeded in zone 1 and the yielding of reinforcement occurred in zone 2, the new structural system of a bridge with joints (in plastic hinge sections) should be considered for designing structural strengthening.

### 3.4. Structural Strengthening of the Bridge

#### 3.4.1. Analysis of Action Effects in Damaged Bridge

Since the nonlinear analysis confirmed plastic hinges formation in the bridge sections in zone 1 and zone 2, a new structural system of the bridge with hinges was formed for the design of structural strengthening of the bridge. The 3D model of the new structural system of the bridge with hinges was formed in the software package [53]. The hinges were modeled at the sections of plastic hinge formations in the main longitudinal girders and in the slab (zone 1 and zone 2). The longitudinal and transverse girders were modeled as linear elements, while the slab was modeled as a shell element. In addition, the river piers and abutments are modeled by shell elements. All structural elements are modeled with actual geometric characteristics, determined for a homogeneous cross-section without

cracks. Action effects from gravity and traffic load were analyzed. The traffic load was calculated for the V-600 type vehicle and the 3.0 m wide traffic lane, according to the existing technical standards for bridge loads [40]. The adopted uniformly distributed load from the V-600 vehicle is 33.3 kN/m<sup>2</sup>. The distributed load in the main traffic lane is 5.0 kN/m<sup>2</sup>, and the uniformly distributed load outside of the main lane is 3.0 kN/m<sup>2</sup>.

In Table 1, a comparison of bending moment demands for the relevant load combination with the bending moment capacities of the main longitudinal girders is presented.

**Table 1.** Comparison of bending moment demands with the bending moment capacities of the main longitudinal girders.

Section	Bending Moment Demands for the Relevant Load Combination (kN·m)	Bending Moment Capacities (kN·m)
At the support S1	18,089	16,000
At the support S2	11,265	16,000
At the support S3	16,617	16,000
In span S01-S1	8025	9112
In span S1-S2	6553	9112
In span S2-S3	10,457	9112
In span S3-S02	11,712	9112

In some cross-sections, the design bending moments are higher than the bending moment capacities. The obtained results clearly indicated the need for structural upgrading of the main longitudinal girders.

In the deck slab, in several cross-sections located in span, capacity moments are slightly exceeded, while at the supports, the slab has a much higher load capacity than required. It was checked and concluded that after the redistribution of action effects, the slab can be considered to have adequate bending capacity.

### 3.4.2. Design of Structural Strengthening

Regarding the damages to the bridge deck, the prestressing technique with cable tendons is selected as the solution for longitudinal girder strengthening. This strengthening method had multiple advantages. Even before the damage, the bridge deck structure did not have adequate resistance according to the currently valid domestic provisions adopted after the construction of the bridge. In addition, the formation of two plastic hinges in the bridge deck structure, after the settlement of the river pier, resulted in a redistribution of action effects with the exceeding of the bending moment capacity in several sections.

The arrangement of cable tendons that favorably affects the load-bearing capacity, balances the bridge system, and ensures its adequate resistance was adopted. Two 15 × 155 mm<sup>2</sup> high-grade steel cable tendons of the BBR VT CONA CMI system [54] with a tensile strength of 1860 MPa are used for prestressing. The tendons are placed along the inside part of the main girder (at the supports in the upper zone and in the spans in the bottom zone). The prestressing cable tendons' layout is linear (see Figure 10). One tendon is adopted along each main girder for the entire bridge length, and another two tendons are added in two damaged middle spans (Figure 10). The prestressing is done from both ends. The steel corrugated pipes are used for tendons installation. The deviators have been placed at the span transverse girders to provide adequate eccentricity of the prestressing force (Figure 11). The tendons are embedded into the corrugated pipes and injected with cement emulsion. At the end supports, the existing transverse girders are strengthened to be able to restrain the tendon forces in the anchoring zone. The steel construction of the deviator is designed for the forces caused by tendons (deflection forces and forces caused by friction forces) in tensioning phase and exploitation state using prescribed safety coefficients.

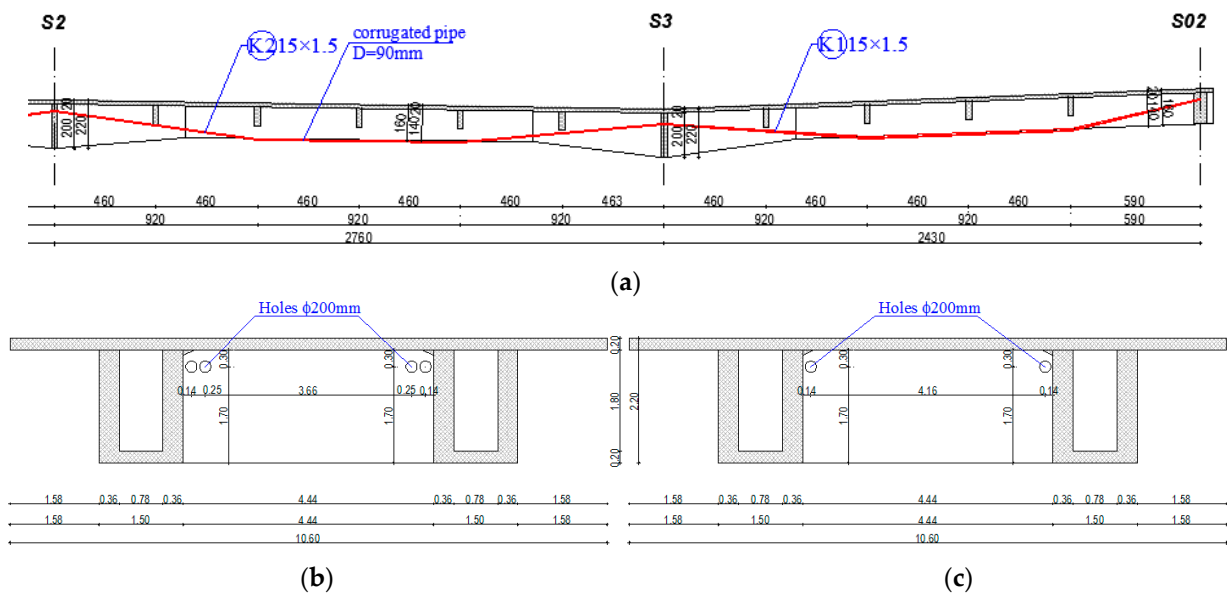


**Figure 10.** Layout of the prestressing cable tendons: (a) longitudinal section (half bridge) and (b) cross-section above piers S2 and S3 and (c) cross-section above pier S1.

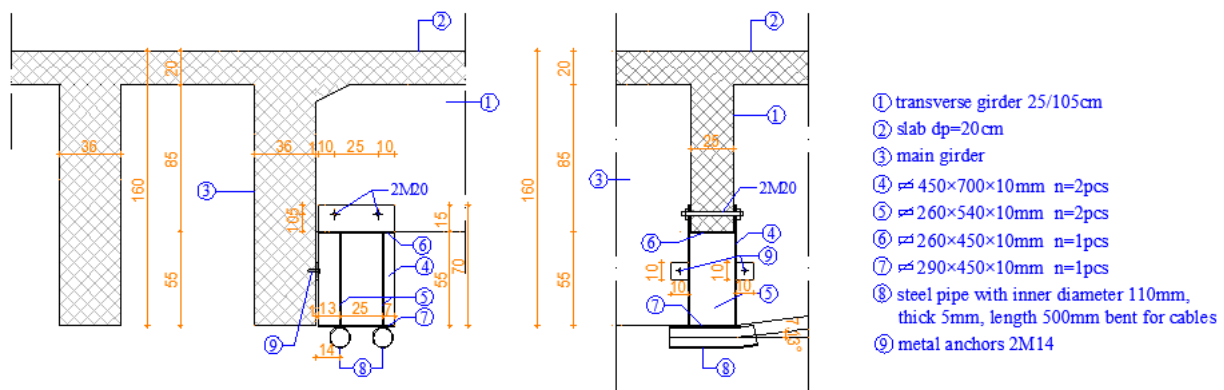


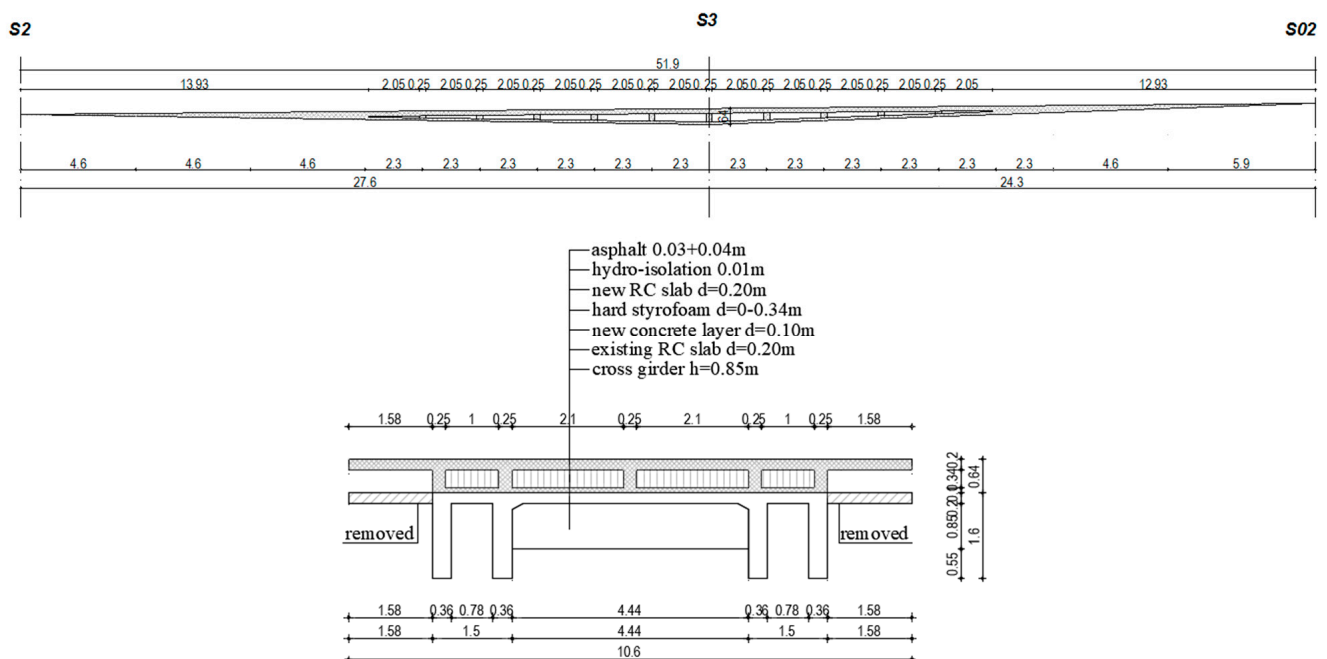
**Figure 11.** Deviator in the span between columns S2-S3 and S3-S02.

For the purpose of verifying the bridge resistance after the adoption of the prestressing cable tendons, a 3D model of the bridge was constructed in the software package TOWER6 [53]. The cables were modeled in the TOWER6 software, taking into account immediate losses (due to friction during cable tension, due to anchoring, and due to the instantaneous deformation of concrete) as well as time-dependent losses. The bending moment demands for the relevant load combination were compared with the capacity moments of the main longitudinal girders for the designed strengthening state (Table 2). For the selected tendons and adopted prestressing forces, the bridge deck structure meets the load-bearing capacity requirements. In addition, the bridge deck structure is strengthened by U-wrapping carbon fibers at the zones of plastic hinge formation for the reason of shear strengthening.

**Table 2.** Comparison of design bending moments with the bending moment capacities of the main longitudinal girders for the designed strengthening state.

Section	Bending Moment Demands for the Relevant Load Combination (kN·m)	Bending Moment Capacities (kN·m)
At the support S1	11,884	16,000
At the support S2	9847	16,000
At the support S3	13,884	16,000
In span S01-S1	5223	9112
In span S1-S2	4974	9112
In span S2-S3	8927	9112
In span S3-S02	7726	9112

In order to form the appropriate longitudinal profile level of the bridge at the place of the pier river settlement, a structure of the RC grill beams with a hard styrofoam filling was designed. The geometry of the RC grill structure is shown in Figure 12. The RC grill structure is designed at the settled part of the bridge (between piers S2-S3-S02). The RC grill structure consists of a 10 cm thick RC concrete layer that is placed over the existing RC slab, four longitudinal girders that follow the geometry of the settled alignment, transverse girders that are placed at a distance of 2.3 m, and an upper new RC slab with a thickness of 0.20 m. The bonding of the newly added grill structure was accomplished with steel anchors drilled into the existing concrete and by applying a coating for the bonding of old and new concrete.

**Figure 12.** The geometry of the RC grill structure.

The foundation of the river settled pier was strengthened by under-concreting and making the RC ring around the existing foundation. Under-concreting was done in camps with the prior cleaning of the degraded rock mass and the installation of anchors for the connection of rock and new concrete. The details of the foundation strengthening are shown in Figure 13.

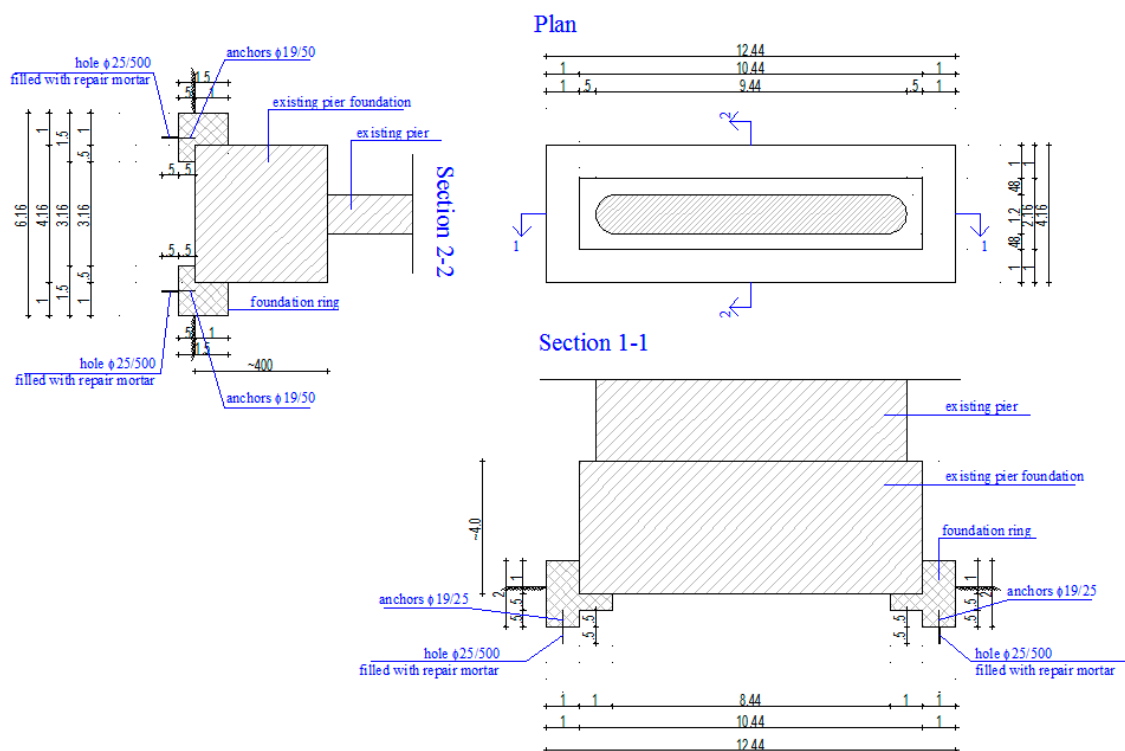


Figure 13. Strengthening of the foundation of river settled pier (units in meters).

#### 4. Damage Assessment of Marsenic Bridge (Bridge 2)

##### 4.1. Description of Bridge Structure

The Marsenic bridge is located in the municipality of Andrijevica. It was built in 1968. The bridge is an RC bridge with a continuous deck system with three spans: 18.0 m, 29.0 m, and 18.0 m, giving a total length of the bridge equal to 65 m. The width of the deck is 3.0 m with two footpaths 0.75 m wide. The bridge is designed with a double-sided longitudinal slope of 2% from the middle to both ends (with a curvature in the middle with a radius of 200.0 m) and a double-sided transverse slope of 2% from the central axis to the footpaths. The longitudinal bridge section, as well as the deck cross-section in the middle of the spans, are shown in Figures 14 and 15.

The bridge deck consists of two girders 0.45 m wide placed at a central distance of 2.95 m. The girders have a variable height from 1.30 m over the abutments to 2.00 m at the middle supports, including the RC slab thickness of 0.20 m. Footpaths are carried by cantilevers 0.75 m long. At the abutments and the river piers, transverse girders with a width of 0.50 m and a height corresponding to the height of the longitudinal girder were designed. In the first and last spans, the transverse girders are 0.25 m thick and 1.20 m high, placed at a distance of 3.60 m, while in the middle span, girders are placed at a central distance of 4.14 m. The river piers are massive concrete elements with a variable cross-section along the height rounded on the upstream and downstream sides. The depth of the piers in the crown is 1.10 m, while at the base is 1.50 m. The width of the piers in the crown is 4.40 m changing to 4.70 m at the base. The foundations of river piers are shallow footings with dimensions of 5.00 × 3.00 × 2.00 m. The abutments are also designed as massive concrete elements with wing walls. The bridge bearings on the abutments are designed as movable neoprene bearings. On the right river pier, a moveable support (RC pendulum) was constructed, while on the left (settled) river pier, a fixed support was designed.

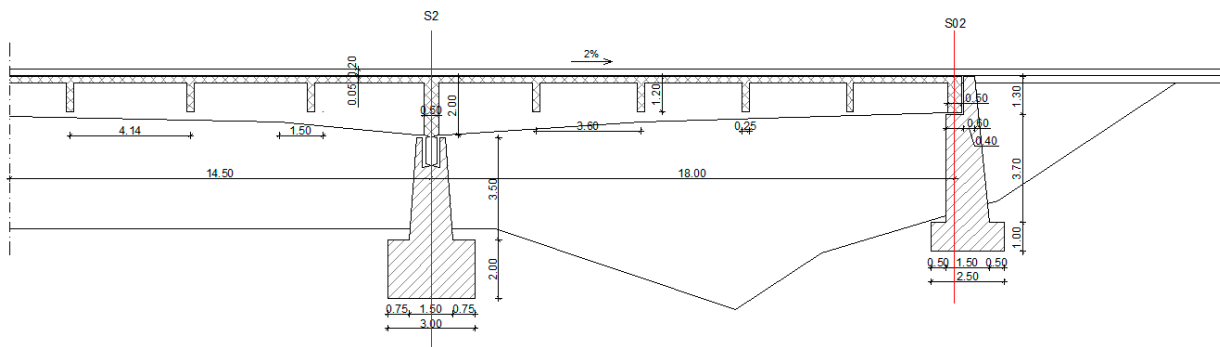


**Figure 14.** The longitudinal section of the bridge 2.

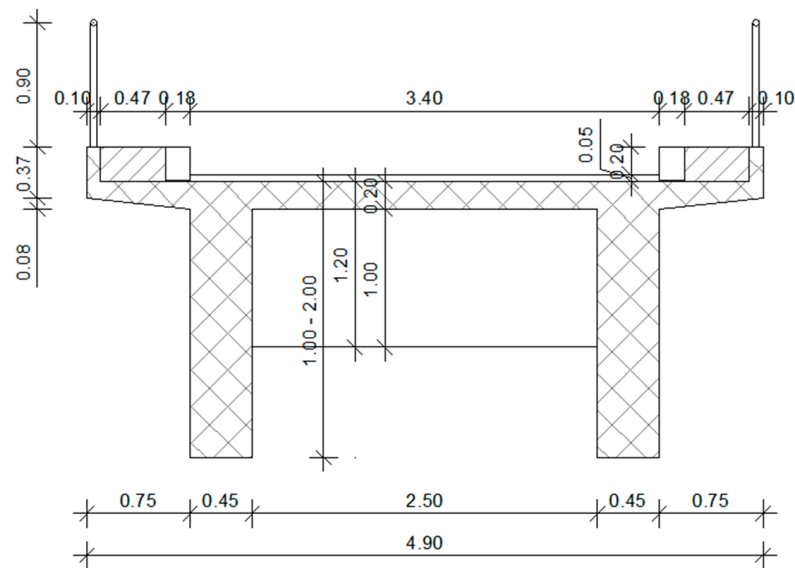


**Figure 15.** The deck cross-section in the middle of the span.

The longitudinal girders are reinforced with 20 $\phi$ 30 in the upper zone at the middle supports, 10 $\phi$ 30 in the bottom zone at the first and last span, and 15 $\phi$ 30 in the bottom zone at the middle span. The foundation of the river piers was done on gravel material. Based on the available design documentation, the solid rock is at a depth of 5 to 6 m.

#### 4.2. Description of Previous Bridge Damage State

Just before the end of the bridge construction (end of 1968), while the bridge deck was still supported by the scaffolding, extensive rainfall happened, which caused reaching maximum water levels (level 1.3 m above the design values). As the scaffolding reduced the water flow profile, the river flow carried the scaffolding out of the middle span, while the left span stayed closed by scaffolding and flood debris and branches. This partially blocked the river channel and diverted the river flow, so the water struck directly on the left pier and caused scouring under the foundation, followed by bridge bents settlement and tilting. As a consequence of this, extensive damage to the bridge deck structure occurred. From that time until 2006, the bridge was in use, despite the damage and a series of reconstruction attempts. The first successful reconstruction of the bridge was done in 2006 [29,55].

Geodetic surveys determined that the total settlement of the left river pier (S1) was 1.16 m. In reconstruction, the settled pier was supported by a foundation on piles. The deck of the bridge was lifted up by 76 cm with hydraulic presses. The deck structure was strengthened by post-tensioned steel tendons (1 + 1 tendon SPB 7 $\phi$ 15.2 mm) placed along the main girders. The existing cracks were injected. One tendon extended along the entire bridge length with a polygonal layout shape, while the other tendon extended only along

the middle span and also with a polytional layout. The right river pier in the reconstruction done in 2006 was not strengthened because in the available design documentation it was written that the foundation of this pier was done on steel piles reaching the solid rock, which proved to be incorrect after new damage occurred in 2010.

#### 4.3. Description of New Bridge Damage State

The extreme river streamflow that occurred in 2010 caused a settlement of the right river pier (S2), based on the geodetic survey, equal to 0.654 m. This settlement caused severe damage to the bridge deck. Above the settled river pier (S2) (zone 1), the cracks about 10 mm wide opened in the girder's bottom zone. The concrete was crushed in the upper zone along the effective footpaths slab width of 0.30 m. Similar damage happened on the deck in the first left span (S01-S1) where cracks appeared in the upper zone (zone 2). On the upstream girder side, a crack 10–13 mm wide appeared at a distance of 10.30 m from the abutment (S01). On the downstream girder side, two cracks 13 mm and 3 mm wide appeared at a distance of 9.78 and 10.95 m from the abutment, respectively. In these sections, concrete crushing occurred in the girder's bottom zone. The scouring was caused by the very high water levels of the river Lim, carrying the flood debris that accumulated at the upstream face of the pier causing increased pressure on the structure and additionally limiting the flow of the water around the bridge. Based on the evaluation of the bridge damage state, it can be concluded that the main causes for the extensive bridge damages were: extreme water level, the inadequate foundation of the pier, and the inadequate water flow profile. The damaged bridge 2 is shown in Figure 16.



(a)



(b)



(c)

**Figure 16.** (a) The bridge after the settlement of the river pier, (b) cracks in zone 1, and (c) cracks in zone 2.

#### 4.4. Nonlinear Analysis of the Bridge 2 Due to the Settlement of the River Pier S2

In order to design the appropriate structural strengthening of the damaged bridge 2 as well as to obtain real action effects in bridge 2 for the new damage state, a nonlinear analysis of bridge 2 due to the settlement of the pier was performed. A schematic representation of the model is shown in Figure 17.

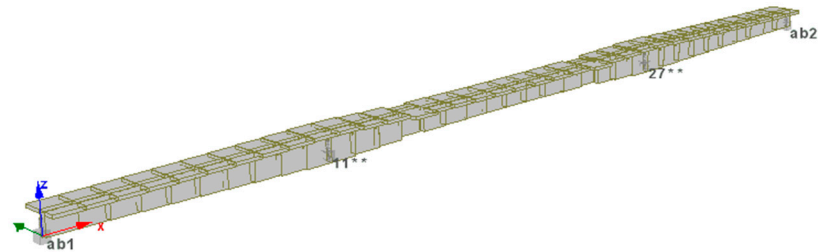


**Figure 17.** Schematic representation of the bridge 2 nonlinear model (\*\* nodes at the bents).

##### 4.4.1. Element Forces during the Analysis

The bridge deck bending moment diagram for several settlement values under the pier S2, including permanent gravity loads, is presented in Figure 18b–d. The initial state shown in Figure 18a refers to permanent gravity loads acting on the deck structure.

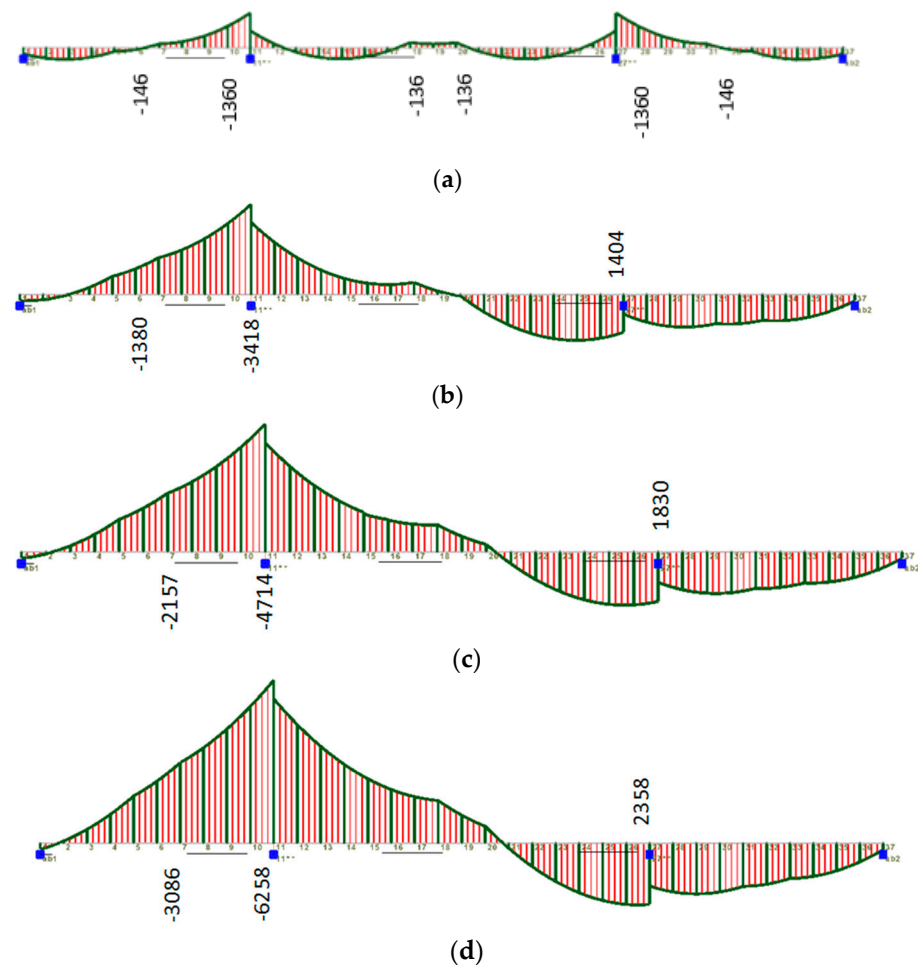


**Figure 18.** (a) Bending moment diagram—initial state (units in kN·m). (b) Bending moment diagram—settlement of 0.08 m under S2 (units in kN·m). (c) Bending moment diagram—settlement of 0.20 m under S2 (units in kN·m). (d) Bending moment diagram—settlement of 0.64 m under S2 (units in kN·m). (\*\* nodes at the bents).

As expected, an increase in negative bending moments at the cross-section above pier S1 up to 4.6 times is noticed, as well as a decrease in negative bending moments at the cross-sections near pier S2 and even their transformation to the positive moments for the significant values of settlement. An increase in bending moments at the upper edge in the first span (S01-S1) is also noted.

#### 4.4.2. Element Deformation and Performance Check

During the loading phases, two performance criteria are defined: reinforcement yield and chord rotation capacity. The reinforcement yield is considered to be reached when reinforcement strain exceeds the value of 0.0012. The chord rotation capacity is calculated based on EN 1998-3:2005 Annex A [48]. The load is applied as displacement below the pier S2 that exhibited foundation settlement in steps of 0.01 m.

The reinforcement yield occurred in the next order: (1) at node 26 located 1.81 m from pier S2, for settlement of S2 pier of 0.08 m; (2) at node 7 located 10.8 m from left abutment S01, for settlement of S2 pier of 0.20 m, (3) at node 6 located 9 m from left abutment S01, for settlement of S2 pier of 0.32 m and (4) at node 5 located 7.2 m from left abutment S01, for settlement of S2 equal to 0.39 m. Chord rotation capacity was reached at node 26 for settlement of S2 pier equal to 0.64 m. Figure 19a–d show a schematic bridge deformed shape at the analysis steps when checked performance criteria are reached.

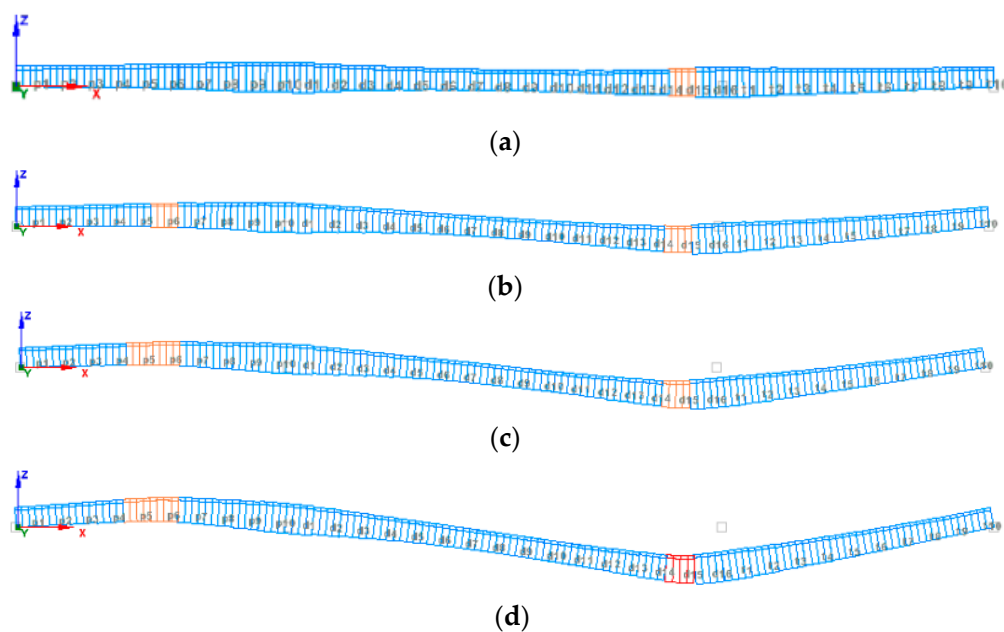


**Figure 19.** (a) Step 9: the reinforcement yield at 1.81 m from S2 pier for 0.08 m settlement of S2 pier. (b) Step 21: the reinforcement yield at 10.8 m from left abutment for 0.20 m settlement of S2 pier. (c) Step 40: the reinforcement yield at 7.2 m from left abutment for 0.39 m settlement of S2 pier. (d) Step 65: the chord rotation capacity reached at 1.81 m from S2 pier for 0.64 m settlement of S2 pier.

Figure 20 shows the bending moment-rotation diagrams for nodes 26 and 7. The points of reaching performance criteria are marked on charts.

Based on the results shown it can be concluded that deck critical sections, located above pier S2 and at the first span, exhibit significant inelastic behavior right after the yielding in reinforcement is detected. Sections of the deck near to pier S2, located at 1.81 m in the inner span, reach the chord rotation capacity (value of 0.018408 rad) at the analysis step that corresponds to the settlement of S2 pier equal to 0.64 m. At this step, the rotation of node 7 is 0.011144 rad, which is 2.5 times less than the rotation capacity of this node. The sections in which significant reinforcement yielding occurred in the nonlinear model (zones of nodes 26 and 7) correspond to the cross-sections in which the damage occurred in the bridge (zone 1 and zone 2). In the zone of node 26 corresponding to zone 1 of bridge damage, the rotation

capacity was reached, which clearly indicates the complete plastification of the plastic hinge. This was obvious from in situ bridge damage in zone 1 where the cracks about 10 mm wide opened in the bottom zone, while the concrete in the upper zone was crushed. In zone 2, where similar damage occurred as in zone 1 but with cracks in the upper zone and crushing of concrete in the bottom zone of the main girders, the plastic hinge formation occurred but rotation capacity was not reached (39% of the rotation capacity was reached). Since the rotation capacities were exceeded in zone 1 and 39% of the capacity was reached in zone 2, the new structural system of the bridge with hinges (in zones of plastic hinge formation) should be considered for designing structural strengthening.

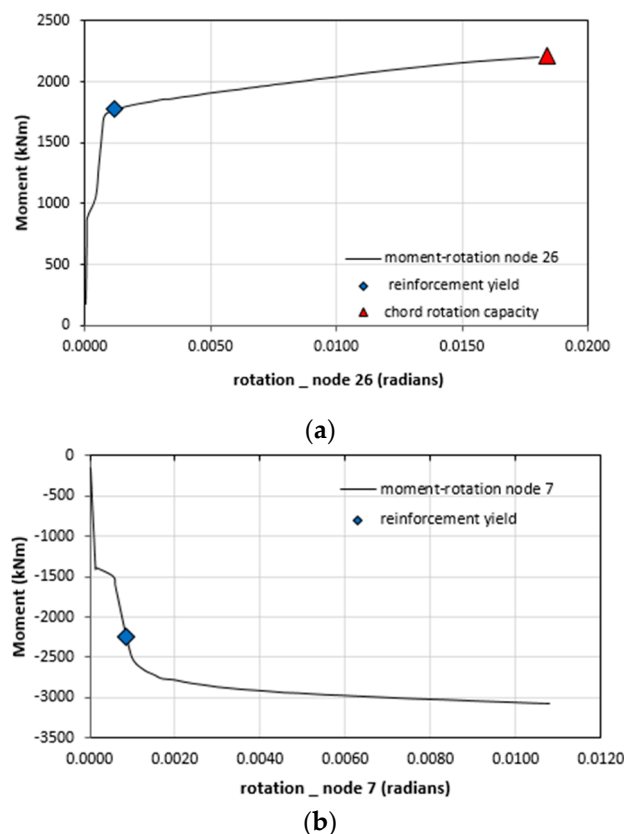


**Figure 20.** Moment rotation curve for nodes (a) 26 and (b) 7.

#### 4.5. Structural Strengthening of the Bridge 2

##### 4.5.1. Element Deformation and Performance Check

Since the nonlinear analysis confirmed plastic hinges formation in the bridge sections in zone 1 and zone 2, a new structural system of the bridge with hinges was built for the design of structural strengthening of the bridge. The 3D model of the new bridge's structural system with hinges was modeled in the software package TOWER6 [53]. The hinges were modeled at the sections of plastic hinge formations in the main longitudinal girders as well as in the slab (zone 1 and zone 2). The longitudinal and transverse girders were modeled as linear elements, while the slab was modeled as a shell element. Additionally, piers and abutments are modeled using shell elements. All bridge elements are modeled with actual geometric characteristics, determined for a homogeneous cross-section without cracks. Action effects from gravity and traffic load were analyzed. The traffic load was calculated for the V-300 type vehicle and the 3.0 m wide traffic lane, according to the existing technical standards for bridge loads [40]. The adopted uniformly distributed load for the V-300 vehicle is 16.67 kN/m<sup>2</sup>. The distributed load in the main traffic lane is 5.0 kN/m<sup>2</sup>, and the uniformly distributed load outside of the main lane is 3.0 kN/m<sup>2</sup>. In Table 3, a comparison of bending moment demands for the relevant load combination with the bending moment capacities of the main longitudinal girders is presented. The main girders meet bending

moment capacity requirements in all sections. No additional bending reinforcement in the RC slab was needed since it was strengthened with prestressing cables in the previous reconstruction (from 2006).

**Table 3.** Comparison of bending moment demands with the bending moment capacities of the main longitudinal girders.

Section	Bending Moment Demands for the Relevant Load Combination (kN·m)	Bending Moment Capacities (kN·m)
At the support S1	4857	6370
At the support S2	1115	6370
In span S01-S1	1362	4085
In span S1-S2	3990	5960
In span S2-S02	2268	4085

#### 4.5.2. Design of Structural Strengthening

Since the deck had sufficient load-bearing capacity for the new damage condition, no additional strengthening was required. The structural strengthening of the settled pier foundation was done by drilled piles. On the upstream and downstream sides of the foundation, 2 RC piles with a diameter of  $\varnothing 80$  and a depth of 9 m were designed. The length of the piles was determined on the basis of available geotechnical data according to which the solid rock is located at a depth of 5–6 m. Each of the piles entered in solid rock at least 2 m. An RC ring was made around the existing foundation. The pile heads are concreted into this ring that with the existing foundation ultimately formed a new pile cap. The coupling of new and old concrete pile caps was performed by the anchors  $\varnothing 19/50$  cm (Figure 21).

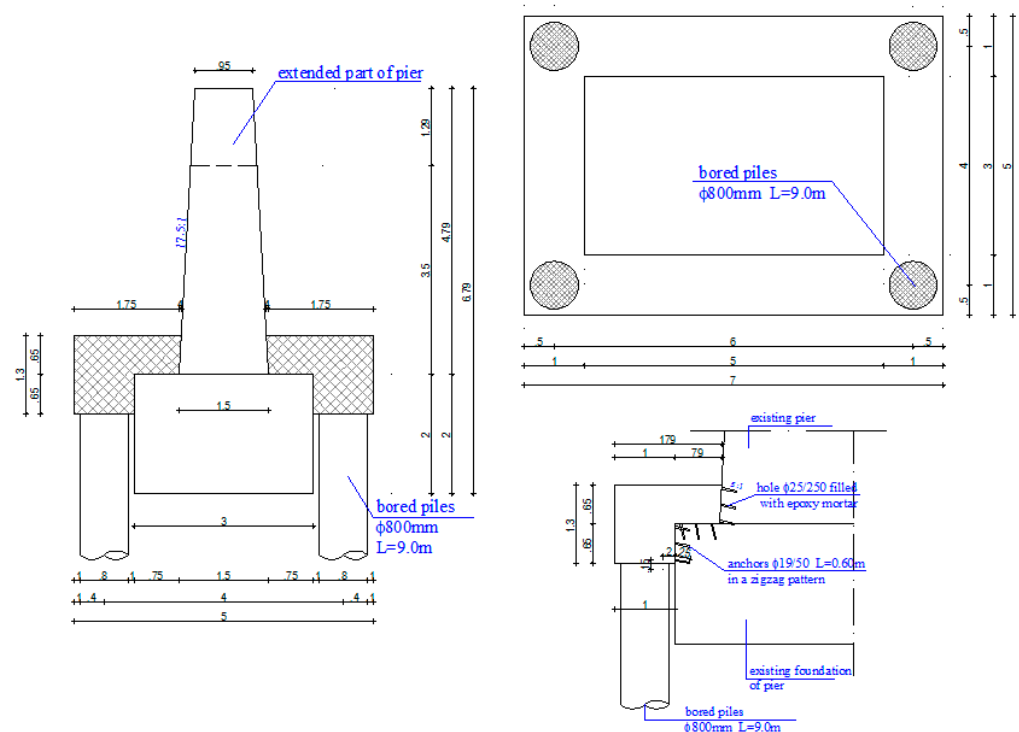


**Figure 21.** Structural strengthening of the settled river pier foundation.

To lift up the deck, the temporary RC supports were made on the right face of the pier, 0.75 to 0.95 m thick and 0.60 m wide. These supports are placed just below the main girders supported at their base by the existing foundation. They are constructed so that their upper edge is 0.50 m from the girder's bottom edge. The existing pendulums are

partially demolished so that temporary supports can be placed under the transverse girders and the pendulums can be removed. Additional pier concreting to the required height is done so that the new bearings can be installed. During the lifting, the deck is transferred to the temporary supports by using the press releasing it from the pendulum at the same time. The pier is concreted to the designed elevation after the deck lifting is completed. After the concrete hardens to at least 70% of the designed strength, moveable bearings are installed, and the bridge deck structure is transferred from temporary to newly installed bearings using hydraulic presses. The temporary supports for presses are removed. The disposition of constructed system for deck structure lifting is shown in Figure 22.

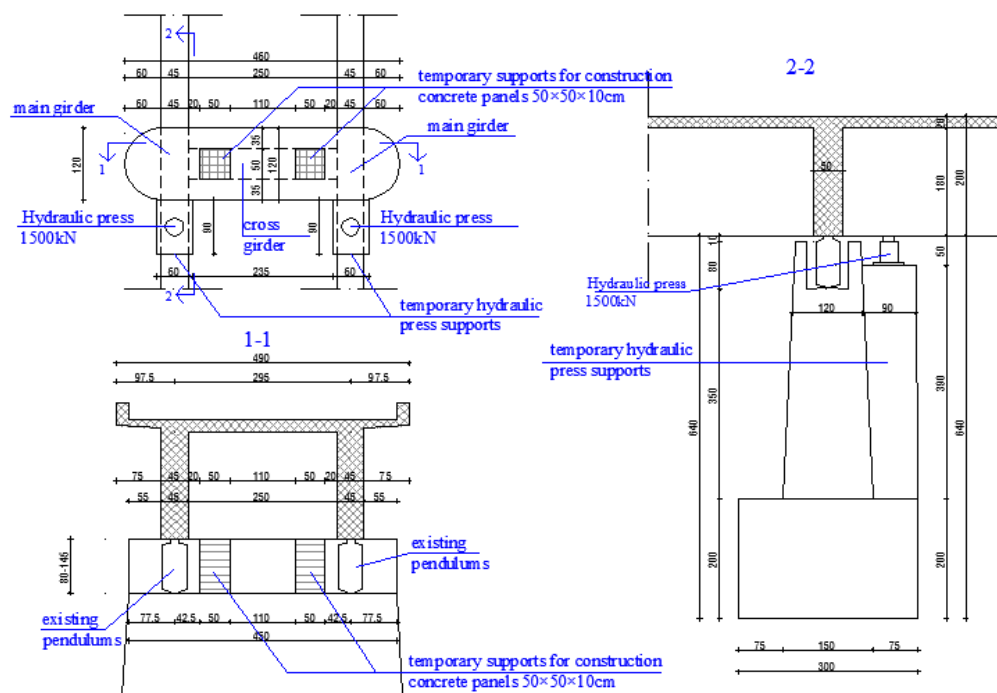


Figure 22. The disposition of constructed system for deck structure raising.

## 5. Damage Assessment of Seoca Bridge (Bridge 3)

### 5.1. Description of Bridge Structure and Bridge Damage State

The Seoca bridge is located on the local road to the village of Seoca in the municipality of Anrijevica. It was built in 2003. The bridge has three spans  $2 \times 18$  m and 6.20 m with a total length of the bridge of 42.20 m. The width of the bridge is 3.0 m. The structural system of the bridge at spans of 18.0 m consists of two prefabricated prestressed girders with a depth of 1.15 m, over which a 0.35 cm thick prefabricated slab is placed. The 6.20 m approaching span was constructed as an RC slab 0.30 m thick and according to the existing design documentation served for high-level water leakage.

The deck supporting structure consists of two abutments and two river piers. The right abutment and right river pier are founded on the rock while the left abutment and the left river pier are founded on gravel. Due to the high water level of the Lim River and the local scour in the foundation of the left pier and left abutment zones, the river flow carried away both these piers as well as the deck over two larger spans of 18 m. Only a deck over a span of 6.20 m remained with the right river pier, right abutment, and the wing walls of the left abutment. The reasons for the collapse of this bridge were inadequate funding of the left river pier and left abutment in combination with extreme water levels and inadequate water flow profile. Figure 23 shows the bridge at its collapse.



**Figure 23.** The Seoca bridge after the collapse.

### 5.2. Designed Reconstruction of the Bridge

Having in mind the causes of the bridge collapse and remaining undamaged bridge elements, at the phase of reconstruction design, a solution for crossing the river Lim with one span, i.e., without river piers was adopted to avoid the negative effects of high water level oscillations. The new bridge structure with one span of 36.00 m was designed. The right-approaching bridge slab with a span of 6.2 m has been retained as part of the new bridge since it was undamaged. The structural system of the new bridge consists of two prefabricated prestressed RC girders with an “I” cross-section of constant height of 1.30 m, placed at a distance of 3.8 m. The longitudinal section and bridge deck cross-section in the middle of the span is shown in Figure 24. These girders are monolithized with a 0.20 m thick RC slab. The flange width (upper and bottom) is 1.00 m, the thickness of the lower flange is from 0.20 to 0.30 m, and the upper flange thickness is from 0.15 to 0.25 m. The thickness of the web is 0.25 m. The prefabricated girders are connected on supports and in the middle of the span with transverse girders 0.30 m wide and 1.10 m high. Over the existing RC approaching slab 0.35 m thick and 3.20 m wide, a new 0.20 m thick and 4.80 m wide RC slab is added over it. At the connection between the new bridge girders and the retained approaching slab, above the pier, a hinge is formed in the slab. The retained right pier is widened to form a suitable support for new prefabricated girders. The existing right abutment has been also retained. The adopted bearings are high-quality elastomeric pot bearings, fixed placed over the right support and moveable placed on the left support. The main girders are prestressed with three  $15 \times 150 \text{ mm}^2$  tendons with a tensile strength of 1860 MPa. The prestressing tendon layouts are linear and parabolic.

Based on the geotechnical survey on the left riverbank, the thickness of the gravel layer above the solid rock is 7.0 m. For these reasons, the left abutment is founded on 1.2 m diameter piles. Two piles placed in the axes of the main girders were designed. The pile cap of  $2.8 \times 1.2 \text{ m}$  was constructed over the piles. The designed length of the piles is 10 m with at least 4.0 m inside the solid rock. The existing wing walls are retained and connected to the new abutment.

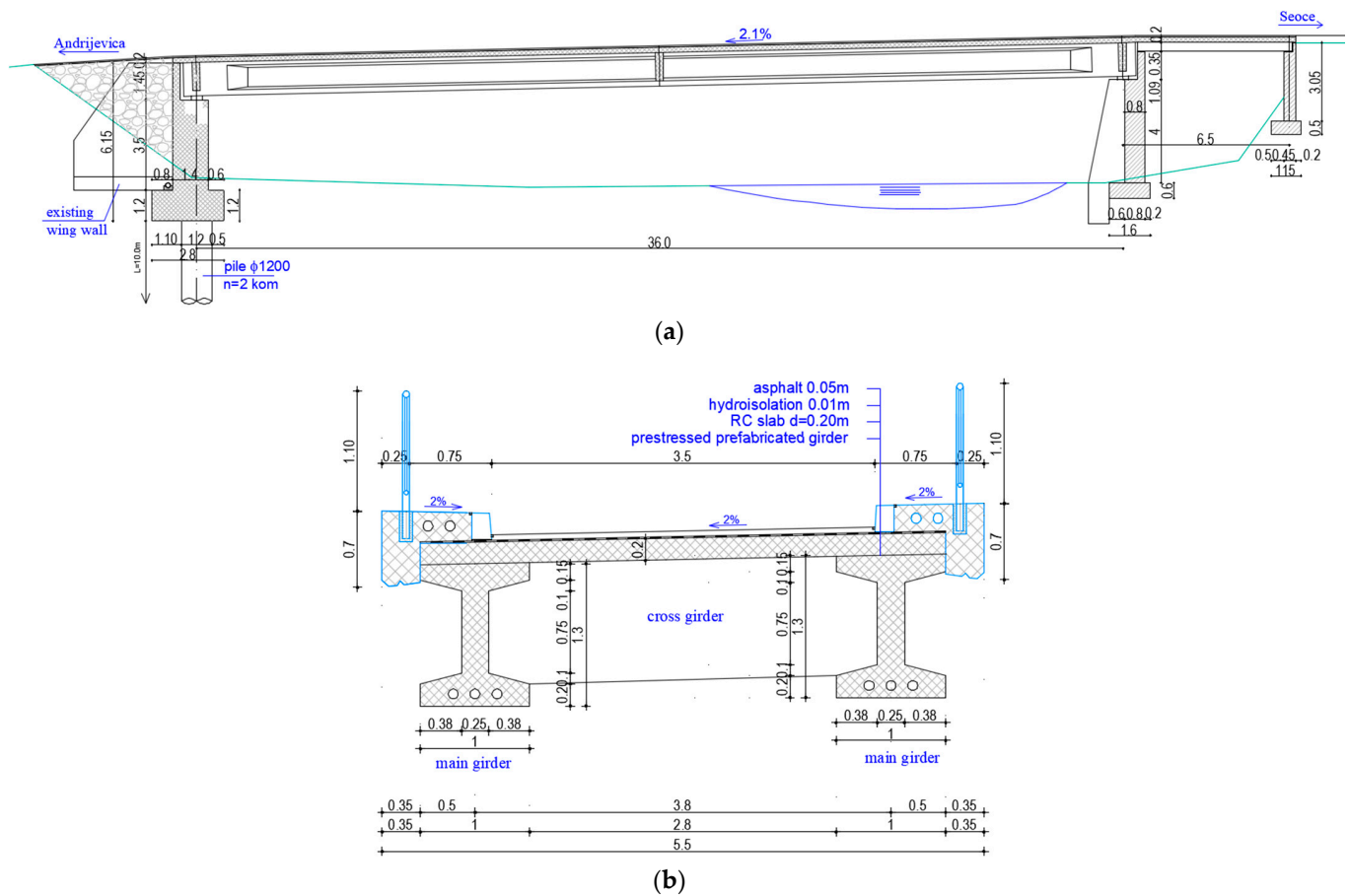


**Figure 24.** The designed reconstruction of the bridge: (a) longitudinal section and (b) cross-section in the middle of the span.

## 6. Damage Assessment of Novsici Bridge in the Municipality of Plav (Bridge 4)

### 6.1. Description of Bridge Structure and Bridge Damage State

The Novsici bridge is located on the local road to the village of Novsici in the municipality of Plav. Since no existing design documentation for this bridge was available, precise data on the bridge structure could not be determined. It was built of reinforced concrete with a span of about 20 m. It had one traffic lane 3.10 m wide with two footpaths of 0.45 m each. The deck structure consisted of two RC main girders with a slab that were placed at a central distance of 2.70 m. The dimensions of the main girders were about  $0.30 \times 1.00$  m. The thickness of the slab could not be determined. During the on-site investigation, it was concluded that the Lim River carried the left abutment as well as the embankment behind it in the width of about 12 to 15 m. The deck structure fell from the left abutment into the riverbed and partially remained supported on the right abutment, so that it stood sloping in the riverbed. No significant damage was noticed in the bridge deck, despite its fall into the riverbed. It is obvious that the left abutment of the collapsed bridge was inadequately founded in gravel, i.e., alluvial sediments, which together with the extreme water level and inadequate flow profile, was the main cause of the bridge collapse. Figure 25 shows the bridge collapse.



**Figure 25.** The Novsici bridge after the collapse.

### 6.2. Designed Reconstruction of the Bridge

Taking into account the causes of the bridge collapse and the current on-site situation, similar to bridge 3, the reconstruction solution by crossing the river Lim with one wider span was selected to avoid the negative effects of high water level oscillations. The bridge with one span of 32.00 m was designed over the river. The longitudinal section of the designed reconstruction of the bridge is shown in Figure 26. The selected structural system of the bridge is the same as for bridge 3 (Figure 24b). In addition, the same supports of the girders are selected. Three  $15 \times 150 \text{ mm}^2$  tendons with a tensile strength of 1860 MPa are used for prestressing. The prestressing tendon layouts are straight and parabolic. Considering the severe damages to the right abutment, a completely new abutment has been designed. All cracked and degraded parts of the rock at this site are removed so that a healthy and solid rock is reached, on which the new abutment is founded. Anchors are drilled into the existing rock to connect the abutment foundation and the rock. The left abutment with wing walls is founded on a rock. In front of and behind the bridge, as well as in the wing zone, the large stone blocks are used to stabilize the slope and prevent erosion.

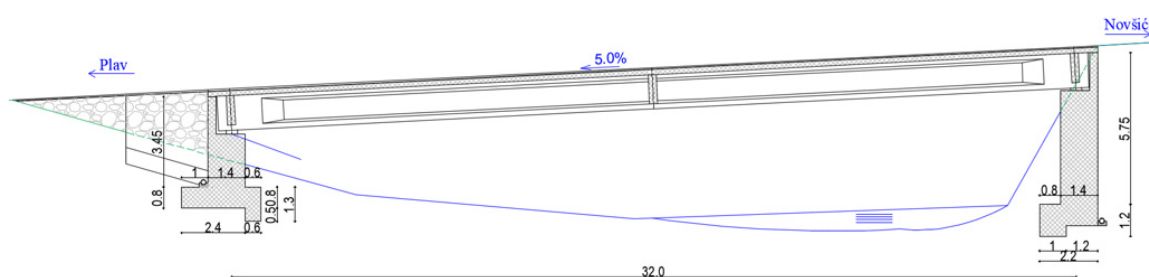


**Figure 26.** Longitudinal section of the designed bridge reconstruction.

## 7. Discussion of the Results

In this paper, a damage assessment of four bridges that were damaged due to extreme river streamflow caused by the Lim River in the zone of 40 km in the municipalities of Plav, Andrijevica, and Berane is presented. Extreme water levels and inadequate flow profiles caused extensive damage to the bridges mostly due to an inadequate pier foundation system. In the case of bridges 1 and 2, scour process in the foundation pier zones and the settlement of river piers (by about 64 cm) happened due to surface erosion and degradation of alluvial sediments. The scouring was caused by the very high water levels of the river Lim, which also carried the flood debris and large tree branches that accumulated at the

upstream face of the piers increasing pressure on the structure and changing river flow. In the case of bridges 3 and 4, the scouring occurred in the abutment foundation zone, which were inadequately founded in gravel deposits or alluvial sediments.

For structural upgrading of bridge 1, the reconstruction solution with prestressed tendons was applied as optimal in terms of safety, resistance, and cost. This reconstruction method is suitable for severely damaged bridge structures where a significant increase in load-bearing capacity is required. For the existing bridge 1, it had multiple advantages. Even before the damage, the bridge deck did not have appropriate load-bearing capacity according to the current regulations for designing bridges adopted after the bridge construction. Additionally, the formation of plastic hinges in the bridge deck, after the river pier settlement, led to a redistribution of action effects in the deck so the ultimate resistance in some sections was exceeded. Such an arrangement of cable tendons in the longitudinal main girders has been designed that favorably affects the load-bearing capacity, balances the bridge system, and ensures its adequate safety. For the selected cable tendons and prestressing forces, the deck bridge structure was provided with sufficient resistance. Unlike bridge 1, for bridge 2, the deck structure had sufficient load-bearing capacity for the new damage state (analyzed on the structural system with hinges), because it was strengthened with prestressed tendons in the previous reconstruction. Therefore, it can be concluded that bridge 2 had more favorable performance under incident load leading to fewer retrofitting actions needed.

The conducted analysis of bridges 1 and 2 performed on nonlinear models, where the structure was exposed to phase settlement, confirmed the real damage state of the bridges and justified the use of a new structural system with hinges in structural strengthening design. On-site measured values of pier settlement match with the values obtained from nonlinear analysis at the state of reaching the rotation capacity (for bridge 1 0.64 m and 0.71 m and for bridge 2 0.654 m and 0.64 m corresponding to measured and numerical values respectively). The zones with extensive damage in the deck correspond to the zones of plastic behavior in the nonlinear model (places of plastic hinge formation). In addition, the achieved levels of hinges plastification in the nonlinear model correspond to the degree of actual bridge damage. It is observed and numerically proven that under severe settlement of piers, damages are concentrated in sections above the settled pier and zone next to the adjacent pier. It is noted that slight shifting of damages towards span happened in bridge 2, which can be explained by the existing span arrangement. In the case of bridge 2, the ratio of outer and inner span length equal to 0.62 is quite at the lower suggested limit, leading to more pronounced negative moments in the middle of the span.

Different from bridge 2 where the deck structure was lifted up with the use of the temporary RC supports, for bridge 1 this was not possible because of fixed supports, so a different solution of bridge leveling was applied. A structure of the RC grill beams with a hard styrofoam filling was designed. The lifting up of the deck of bridge 2 was done with the hydraulic presses by which the deck is first placed on the temporary supports and after to the newly installed bearings. The piers were also concreted to the required height so that the bearings could be installed.

For bridge 1, the deep foundation reconstruction of the settled river pier was not needed, while the settled river pier of bridge 2 required a foundation on piles. Based on the available geotechnical data, the solid rock was at a depth of 5 to 6 m, so two RC piles with a diameter of  $\varnothing 800$  mm and a depth of 9 m were designed.

For bridges 3 and 4, taking into account the causes of damage, reconstruction solutions have been designed such that the Lim River is crossed by one wider span or without a pier in the riverbed to avoid the negative effects of high water level oscillations. A solution with two prestressed RC girders of the "I" cross-section, monolithized with RC slab and with high-quality elastomeric pot bearings, on one side fixed and movable on the other side, was designed. For bridge 3, where a thicker gravel layer above the rock existed, it was necessary to design the left abutment foundation on piles with a diameter of  $\varnothing 1200$  mm 10 m deep, while the abutments of bridge 4 did not require a deep foundation. In the case of bridge 4,

a completely new right abutment was designed, while all cracked and degraded parts of the rock mass were removed in order to reach a healthy and solid rock.

## 8. Conclusions

This paper presents a damage analysis and assessment of several bridges in Montenegro (selected as prototypes) that were heavily damaged due to extreme river streamflow. Since no comprehensive study on the vulnerability of existing deteriorated bridges to the extreme river stream conditions has been conducted in Montenegro, although almost 60 bridges were built in the Lim River basin area, the conducted study presented in this paper partially fills an existing gap. The findings obtained on selected prototype bridges can be used in the vulnerability assessment and reconstruction planning phase for other bridges in the subject zone, to determine design and construction flaws, vulnerable bridge components, possible retrofitting technics, and retrofitting design assumptions proven to be efficient.

It is concluded that the main reason for the bridge damage for all analyzed bridges was that they have not been adequately founded. Commonly applied shallow foundations on degraded rock or in gravel in the riverbed were proven to be bad design solutions in high water level oscillation conditions (over 100 times). Additionally, based on the studies presented here, inadequately provided water flow profiles were the reason for bridge collapses. The detected vulnerable zones in analyzed bridges, also numerically justified, were located in deck sections above the piers that settled as well as in zones next to the adjacent pier. It is proven that in the retrofitting design of damaged bridges, the use of a new structural system with hinges inserted in zones where significant damage was observed is an adequate design assumption. Previously strengthened bridge structure by deck prestressing, was proven to have more favorable failure performance due to extreme pier settlement since deck capacity was not reached in new damage state (analyzed on the structural system with hinges). The deep foundation of piers and deck prestressing were the most commonly applied retrofitting techniques, which assured a significant increase in the load-bearing capacity of the bridge structure as well as its durability.

**Author Contributions:** Conceptualization, J.P., N.S. and R.P.; methodology, J.P., N.S. and R.P.; software, J.P. and N.S.; validation, J.P., N.S. and R.P.; formal analysis, J.P., N.S. and R.P.; investigation, J.P., N.S. and R.P.; resources, R.P.; data curation, R.P.; writing—original draft preparation, J.P., N.S. and R.P.; writing—review and editing, J.P., N.S. and R.P. All authors have read and agreed to the published version of the manuscript.

**Funding:** This research received no external funding.

**Conflicts of Interest:** The authors declare no conflict of interest.

## References

1. Mitoulis, S.A.; Argyroudis, S.A.; Loli, M.; Imam, B. Restoration models for quantifying flood resilience of bridges. *Eng. Struct.* **2021**, *238*, 112180. [[CrossRef](#)]
2. Kirby, A.M.; Roca, M.; Kitchen, A.; Escarameia, M.; Chesterton, O.J. *Manual on Scour at Bridges and Other Hydraulic Structures*, 2nd ed.; CIRIA Report C742; CIRIA: London, UK, 2015.
3. Gidaris, I.; Padgett, J.E.; Barbosa, A.R.; Chen, S. Multiple-Hazard Fragility and Restoration Models of Highway Bridges for Regional Risk and Resilience Assessment in the United States: State-of-the-Art Review. *J. Struct. Eng.* **2017**, *143*, 04016188. [[CrossRef](#)]
4. Alipour, A.; Shafei, B. Performance assessment of highway bridges under earthquake and scour effects. In Proceedings of the 15th World Conference on Earthquake Engineering, Lisbon, Portugal, 24–28 September 2012.
5. Alipour, A.; Shafei, B.; Shinozuka, M. Reliability-based calibration of load and resistance factors for design of RC bridges under multiple extreme events: Scour and earthquake. *J. Bridge Eng.* **2013**, *18*, 362–371. [[CrossRef](#)]
6. Banerjee, S.; Prasad, G.G. Seismic risk assessment of reinforced concrete bridges in flood-prone regions. *Struct. Infrastruct. Eng.* **2013**, *9*, 952–968. [[CrossRef](#)]
7. Prasad, G.G.; Banerjee, S. The impact of flood-induced scour on seismic fragility characteristics of bridges. *J. Earthq. Eng.* **2013**, *17*, 803–828. [[CrossRef](#)]

8. Wang, Z.; Dueñas-Osorio, L.; Padgett, J.E. Influence of scour effects on the seismic response of reinforced concrete bridges. *Eng. Struct.* **2014**, *76*, 202–214. [[CrossRef](#)]
9. Wang, Z.; Padgett, J.E.; Dueñas-Osorio, L. Risk-consistent calibration of load factors for the design of reinforced concrete bridges under the combined effects of earthquake and scour hazards. *Eng. Struct.* **2014**, *79*, 86–95. [[CrossRef](#)]
10. Yilmaz, T.; Banerjee, S.; Johnson, P.A. Performance of two real-life California bridges under regional natural hazards. *J. Bridge Eng.* **2016**, *21*, 04015063. [[CrossRef](#)]
11. Gehl, P.; D’Ayala, D. Development of Bayesian networks for the multi-hazard fragility assessment of bridge systems. *Struct. Saf.* **2016**, *60*, 37–46. [[CrossRef](#)]
12. Masjedi, A.; Bejestan, M.S.; Kazemi, H. Effects of Bridge Pier Position in a 180 Degree Flume Bend on Scour Hole Depth. *J. Appl. Sci.* **2010**, *10*, 670–675. [[CrossRef](#)]
13. Diehl, T.H. *Potential Drift Accumulation at Bridges*; U.S. Department of Transportation, Federal Highway Administration: Richmond, VA, USA, 1997.
14. Wardhana, K.; Hadipriono, F.C. Analysis of Recent Bridge Failures in the United States. *J. Perform. Constr. Facil.* **2003**, *17*, 144–150. [[CrossRef](#)]
15. Cook, W.; Barr, P.J.; Halling, M.W. Bridge Failure Rate. *J. Perform. Constr. Facil.* **2015**, *29*, 04014080. [[CrossRef](#)]
16. World Bank Group. Serbia Floods 2014. Available online: [http://www.sepa.gov.rs/download/SerbiaRNAreport\\_2014.pdf](http://www.sepa.gov.rs/download/SerbiaRNAreport_2014.pdf) (accessed on 1 December 2021).
17. Ju, S.H. Determination of scoured bridge natural frequencies with soil–structure interaction. *Soil Dyn. Earthq. Eng.* **2013**, *55*, 247–254. [[CrossRef](#)]
18. Prendergast, L.J.; Hester, D.; Gavin, K.; O’Sullivan, J.J. An investigation of the changes in the natural frequency of a pile affected by scour. *J. Sound Vib.* **2013**, *332*, 6685–6702. [[CrossRef](#)]
19. Klinga, J.V.; Alipour, A. Assessment of structural integrity of bridges under extreme scour conditions. *Eng. Struct.* **2015**, *82*, 55–71. [[CrossRef](#)]
20. Kim, H.; Sim, S.H.; Lee, J.; Lee, Y.J.; Kim, J.M. Flood fragility analysis for bridges with multiple failure modes. *Adv. Mech. Eng.* **2017**, *9*. [[CrossRef](#)]
21. Prendergast, L.J.; Gavin, K. A review of bridge scour monitoring techniques. *J. Rock Mech. Geotech. Eng.* **2014**, *6*, 138–149. [[CrossRef](#)]
22. Maroni, A.; Tubaldi, E.; Douglas, J.; Ferguson, N.; Val, D.; McDonald, H.; Lothian, S.; Chisholm, A.; Riches, O.; Walker, D.; et al. Managing Bridge Scour Risk Using Structural Health Monitoring. In *International Conference on Smart Infrastructure and Construction (ICSIC)*; ICE Publishing: London, UK, 2019; pp. 77–84. [[CrossRef](#)]
23. Boujia, N.; Schmidt, F.; Chevalier, C.; Siegert, D.; Pham van Bang, D. Effect of Scour on the Natural Frequency Responses of Bridge Piers: Development of a Scour Depth Sensor. *Infrastructures* **2019**, *4*, 21. [[CrossRef](#)]
24. Pejovic, R.; Mijuskovic, O.; Kapor, V. Bridge repair over the river pčinja on the primary road podgorica–kolašin. In *Sanacija Mosta Preko Rijeke Pčinje na Magistralnom Putu Podgorica–Kolašin, Proceedings of the 1st International Conference “Civil Engineering—Science & Practice” GNP 2006 (Book 2)*; Faculty of Civil Engineering, University of Montenegro: Žabljak, Montenegro, 2006; pp. 669–676. ISBN 86-82707-13-6. (In Montenegrin)
25. Pejovic, R.; Blagojevic, J.; Blagojevic, R.; Matijasevic, S.; Prascevic, V. Reconstruction and rehabilitation of the bridge “mojkovac” over juškovića river. In *Rekonstrukcija i Sanacija Mosta “Mojkovac” Preko Juškovića Potoka, Proceedings of the 3rd International Conference “Civil Engineering—Science & Practice” GNP 2010 (Book 1)*; Faculty of Civil Engineering, University of Montenegro: Žabljak, Montenegro, 2010; pp. 365–370. ISBN 978-86-82707-18-9. (In Montenegrin)
26. Pejovic, R.; Blagojevic, J.; Pejovic, J.; Serdar, N. *Reconstruction of the Plav Bridge on the Regional Road R-9 Murino-Plav-Gusinje. Rekonstrukcija Plavskog Mosta na Regionalnom Putu R-9 Murino-Plav-Gusinje*; Osmo Naučno-Stručno Savjetovanje: Ocjena Stanja, Održavanje i Sanacija Građevinskih Objekata i Naselja; Savez Građevinskih Inženjera Srbije: Zlatibor, Serbia, 2013. (In Montenegrin)
27. Pejovic, R.; Blagojevic, J.; Blagojevic, R.; Tasevski, D.; Pejovic, J.; Matijasevic, S.; Prascevic, V. *Reconstruction of the Blažo Jovanović Bridge over the Morača River in Podgorica. Rekonstrukcija Mosta Blaža Jovanovića Preko Rijeke Morače u Podgorici*; VI Naučno-Stručni skup, Savremena Teorija i Praksa u Graditeljstvu, Zbornik Radova; Ministarstvo za Prostorno Uređenje Građevinarstvo i Ekologiju Vlade Republike Srpske, Arhitektonsko-Građevinski Fakultet Banja Luka, Privredna Komora Republike Srpske i Zavod za Izgradnju A.D.: Banja Luka, Srpska; Bosnia, Srpska; Herzegovina, Srpska, 2010; pp. 343–352, ISBN 978-99955-630-5-9. (In Montenegrin)
28. Pejovic, R.; Tasevski, D.; Mihailovska, J.; Blagojevic, J.; Blagojevi, R. *Reasons of Damages and Durability of Concrete Bridges. Uzroci Oštećenja i Trajnost Betonskih Mostova*; IX Naučno-Stručno Savjetovanje, Ocjena stanja, Održavanje i Sanacija Građevinskih Objekata i Naselja; Savez Građevinskih Inženjera Srbije: Zlatibor, Serbia, 2015. (In Montenegrin)
29. Pejovic, R.; Kapor, V. *Rehabilitation of the Bridge Marsenic over the River Lim. Sanacija Mosta Preko Rijeke Lim kod Rijeke Marsenića*; V naučno-Stručno Savjetovanje, Ocena Stanja, Održavanje i Sanacija Građevinskih Objekata i Naselja, Zbornik Radova; IT-Savez Inženjera i Tehničara Srbije: Zlatibor, Serbia, 2007; pp. 91–96, ISBN 987-86-904089-3-1. (In Montenegrin)
30. *Privremeni Tehnički Propisi za Beton i Armirani Beton (Temporary Technical Regulations for Concrete and Reinforced Concrete)*; PTP-3; Ministarstvo Građevine FNRJ; Belgrade, Yugoslavia, 1947.
31. *Privremeni Tehnički Propisi za Određivanje Veličine Opterećenja na Mostovima (Temporary Technical Regulations for Determining the Load on Bridges)*; PTP-5; Ministarstvo Građevine FNRJ; Belgrade, Yugoslavia, 1947.

32. Imperatore, S.; Rinaldi, Z.; Spagnuolo, S. Experimental investigations on the effects of the steel rebar corrosion at structural level. *Struct. Concr.* **2019**, *20*, 2230–2241. [[CrossRef](#)]
33. Bossio, A.; Imperatore, S.; Kioumarsis, M. Ultimate Flexural Capacity of Reinforced Concrete Elements Damaged by Corrosion. *Buildings* **2019**, *9*, 160. [[CrossRef](#)]
34. Castel, A.; Francois, R.; Arligue, G. Mechanical behavior of corroded reinforced concrete beams—Part 1: Experimental study of corroded beams. *Mater. Struct.* **2000**, *33*, 539–544. [[CrossRef](#)]
35. Coronelli, D.; Gambarova, P. Structural assessment of corroded reinforced concrete beams: Modeling guidelines. *J. Struct. Eng.* **2004**, *130*, 1214–1224. [[CrossRef](#)]
36. Carlo, F.D.; Meda, A.; Rinaldi, Z. Numerical evaluation of the corrosion influence on the cyclic behavior of RC columns. *Eng. Struct.* **2017**, *153*, 264–278. [[CrossRef](#)]
37. Meda, A.; Mostosi, S.; Rinaldi, Z.; Riva, P. Experimental evaluation of the corrosion influence on the cyclic behavior of RC columns. *Eng. Struct.* **2014**, *76*, 112–123. [[CrossRef](#)]
38. Rinaldi, Z.; Imperatore, S.; Valente, C. Experimental evaluation of the flexural behavior of corroded P/C beams. *Constr. Build. Mater.* **2010**, *24*, 2267–2278. [[CrossRef](#)]
39. Rinaldi, Z.; Valente, C.; Pardi, L. A simplified methodology for the evaluation of the residual life of corroded elements. *Struct. Infrastruct. Eng.* **2008**, *4*, 139–152. [[CrossRef](#)]
40. *Rulebook on Technical Standards for Determining Bridge Loads*; Official Gazette of the SFRJ, No. 1/91; Belgrade, Serbia, 1990; 20p. Available online: [http://demo.paragraf.rs/demo/combined/Old/t/t2004\\_07/t07\\_0001.htm](http://demo.paragraf.rs/demo/combined/Old/t/t2004_07/t07_0001.htm) (accessed on 1 February 2011).
41. *EN1992-1-1*; Design of Concrete Structures. Part 1: General Rules and Rules for Buildings. European Committee for Standardization: Brussels, Belgium, 2004.
42. *EN1998-2*; Design of Structures for Earthquake Resistance Part 2: Bridges. European Committee for Standardization: Brussels, Belgium, 2005.
43. *EN1991-2*; Actions on Structures—Part 2: Traffic Loads on Bridges. European Committee for Standardization: Brussels, Belgium, 2003.
44. Brandimarte, L.; Paron, P.; Baldassarre, G.D. Bridge pier scour: A review of processes, measurements and estimates. *Environ. Eng. Manag. J.* **2012**, *11*, 975–989. [[CrossRef](#)]
45. Kuspilić, N.; Gilja, G. Influence of watercourse flow on bridge safety. *e-Zb. Elektron. Zb. Rad. Građevinskog Fak.* **2018**, *8*, 24–38.
46. Tmusic, L.; Perović, Z. Ministarstvo Unutrašnjih Poslova—Direktorat za Zaštitu i Spašavanje. Procjena Rizika od Katastrofa Crna Gora. 2021; ISBN 978-9940-8815-1-1. Available online: <https://media.gov.me/media/gov/2021/mup/nacionalna-procjena-rizika-elektronska-publikacija.pdf> (accessed on 1 December 2021).
47. SeismoStruct v.7.0.3. Seismosoft, Softver for Static and Dynamic Structural Analysis. 2014. Available online: <https://seismosoft.com> (accessed on 1 December 2021).
48. Helleland, J.; Scordelis, A. *Analysis of RC Bridge Columns under Imposed Deformations*; IABSE Colloquium: Delft, The Netherlands, 1981; pp. 545–559.
49. Mari, A.; Scordelis, A. *Nonlinear Geometric Material and Time Dependent Analysis of Three Dimensional Reinforced and Prestressed Concrete Frames*; SESM Report 82-12; Department of Civil Engineering, University of California: Berkeley, CA, USA, 1984.
50. Mander, J.B.; Priestley, M.J.N.; Park, R. Theoretical stress-strain model for confined concrete. *J. Struct. Eng.* **1988**, *114*, 1804–1826. [[CrossRef](#)]
51. Menegotto, M.; Pinto, P.E. Method of Analysis for Cyclically Loaded RC Plane Frames, Including Changes in Geometry and Non-Elastic Behavior of Elements Under Combined Normal Force and Bending. In Proceedings of the IABSE Symposium on Resistance and Ultimate Deformability of Structures Acted on by Well Defined Repeated Loads, Lisbon, Portugal, 1973.
52. *EN1998-3*; Design of Structures for Earthquake Resistance—Part 3: Assessment and Retrofitting of Buildings. European Committee for Standardization: Brussels, Belgium, 2005.
53. *TOWER6. Software for Static and Dynamic Structural Analysis, Concrete, Steel and Timber Design*; Radimpex: Belgrade, Serbia, 2010; Available online: <https://mail.radimpex.rs/en/tower> (accessed on 1 February 2011).
54. BBR VT CONA CMI-Bonded PT System, BBR VT International Ltd. 2006. Available online: [http://www.bbrnetwork.com/aboutus/news/singleview/article/bbr\\_vt\\_cona\\_cmi\\_bonded\\_pt\\_system.html](http://www.bbrnetwork.com/aboutus/news/singleview/article/bbr_vt_cona_cmi_bonded_pt_system.html) (accessed on 1 December 2021).
55. Pejovic, R. *Glavni i Izvođački Projekat Sanacije Mosta Preko Rijeke Lim kod Rijeke Marsenića. Main Design of the Rehabilitation for the Bridge Marsenic over the River Lim*; Faculty of Civil Engineering: Rijeka, Croatia, 2006.